FRAGMENTATION POTENTIAL FOR THE TERNARY DECAY OF ^{252}Cf

BY

DEEPA.G

(11PHS03)

A dissertation submitted to the

AVINASHILINGAM INSTITUTE FOR HOME SCIENCE AND HIGHER EDUCATION FOR WOMEN - UNIVERSITY

COIMBATORE – 641 043.

In partial fulfilment of the requirements for the degree of

MASTER OF SCIENCE IN PHYSICS

MAY 2013

FRAGMENTATION POTENTIAL FOR THE TERNARY DECAY OF ^{252}Cf

BY

DEEPA.G

(11PHS03)

A dissertation submitted to the

AVINASHILINGAM INSTITUTE FOR HOME SCIENCE AND HIGHER EDUCATION FOR WOMEN - UNIVERSITY COIMBATORE – 641 043.

In partial fulfilment of the requirements for the degree of

MASTER OF SCIENCE IN PHYSICS

MAY 2013

CERTIFIED AS A BONAFIDE RESEARCH WORK

10.5.13

Signature of the

Head of the Department

10/5/2013

Signature of the Guide

ACKNOWLEDGEMENT

I wish to express my deep sense of reverential gratitude to **Thiru. T.S.K.Meenakshi Sundharam,** Chancellor, Avinashilingam Institute for Home Science and Higher Education for Women, Coimbatore, for providing the facilities to conduct this study.

I sincerely thanks to **Dr. (Tmt.) Sheela Ramachandran**, M.Sc, P.G. Dip., PhD., Vice Chancellor, Avinashilingam Institute for Home Science and Higher Education for Women, Coimbatore, for providing flamboyant help towards the completion of the study.

I extend my thanks to **HON.COL. (Tmt.) Saroja Prabhakaran,** M.A., Dip.Ed., Ph.D., former Vice Chancellor, , Avinashilingam Institute for Home Science and Higher Education for Women, Coimbatore, for the moral support, kind blessing and providing the adequate help required to carry out the study.

I record my deep sense of gratitude and indebtedness to **Dr. (Tmt.) Gowri Ramakrishnan,** M.Sc., M.Phil., Ph.D., Registrar, Avinashilingam Institute for Home Science and Higher Education for Women, Coimbatore, for providing adequate help for the study.

I also wish to express my gratitude to **Dr. (Tmt.) R. Parvatham,** M.Sc., Dip.Ed., M.Phil., Ph.D., Dean, Faculty of Science, Avinashilingam Institute for Home Science and Higher Education for Women, Coimbatore, for timely help rendered throughout the course.

I wholeheartedly thank **Dr. (Tmt.) Rachel Oommen,** M.Sc., Dip. Ed., B.Ed., M.Phil., Ph.D., Professor and Head of the Department of Physics, Avinashilingam Institute for Home Science and Higher Education for Women, Coimbatore, for her encouragement.

I am very much indebted to my guide **Tmt. N.S. Rajeswari** M.Sc., M.Phil., M.C.A., Assistant Professor, Department of Physics, Avinashilingam Institute for Home Science and Higher Education for Women, Coimbatore, for her excellent, outstanding guidance, constructive critism, motivation, valuable advice, untiring support, timely suggestions, holding me strong in all the places I faltered.

I extend my thanks to **Dr. M. Balasubramaniam,** Assistant Professor, Department of Physics, Bharathiar University, Coimbatore, for his advice and guidance rendered throughout the study to its zenith.

I sincerely thank all the **staff members** of the Department of Physics, Avinashilingam Institute for Home Science and Higher Education for Women, Coimbatore, for being supportive and understanding.

And I thank all my **friends** for their support, understanding and co-operation for the successful completion of the study.

Deepa.G

CONTENTS

CHAPTER No.	TITLE	PAGE No.
	LIST OF FIGURES	
I	**INTRODUCTION**	**1-15**
	1.1 Introduction	
	1.2 Basic Fission Model	
	1.3 Fission process	
	1.4 Spontaneous Fission	
	1.5 Induced Fission	
	1.6 Fission products	
	1.7 Energy and charge distribution of fission products	
	1.8 Mass distribution of fission products	
	1.9 Binary Fission	
	1.10 Ternary Fission (TF)	
	1.11 Mechanism of Ternary Fission	
	1.12 Cold and Hot Ternary Fission	
	1.13 Models of Ternary Fission	
	1.14 Cluster and Ternary Fission	
	1.15 Objectives of the study	
	References	

II	**REVIEW OF LITERATURE**	**16 - 32**
	2.1 Introduction	
	2.2 Review on theoretical studies on Ternary Fission of ^{252}Cf	
	2.3 Review on experimental studies on Ternary Fission of ^{252}Cf	
	References	
III	**METHODOLOGY**	**33-40**
	3.1 Introduction	
	3.2 Binding Energy	
	3.3Mass Asymmetry	
	3.4 Coulomb potential	
	3.5 Proximity potential	
	3.6 Model	
	3.7 Three cluster model (TCM)	
	References	
IV	**RESULTS AND DISCUSSION**	**41 - 62**
	4.1 He accompanied Ternary Fission	
	4.2 Be accompanied Ternary Fission	
	4.3 C accompanied Ternary Fission	
	4.4 Mg accompanied Ternary Fission	
	4.5 ^{3}He, ^{10}Be, ^{14}C, ^{27}Mg accompanied Ternary Fission.	
	References	
V	**SUMMARY AND CONCLUSION**	**63**

LIST OF FIGURES

FIGURE NO.	TITLE	PAGE NO.
1.1	Steps in the process of nuclear fission according to the liquid drop model.	12
1.2	Potential energy during different stages of fission.	13
1.3	Schematic touching configuration of the spherical nuclei in Ternary Fission.	13
3.1	Schematic touching configuration in the case of collinear emission.	39
4.1	Fragmentation potential plotted with respect to A_2 for ^{3}He fixed as a third particle.	45
4.2	Fragmentation potential plotted with respect to A_2 for ^{4}He fixed as a third particle.	45
4.3	Fragmentation potential plotted with respect to A_2 for ^{5}He fixed as a third particle.	46
4.4	Fragmentation potential plotted with respect to A_2 for ^{6}He fixed as a third particle.	46
4.5	Fragmentation potential plotted with respect to A_2 for ^{7}He fixed as a third particle.	47
4.6	Fragmentation potential plotted with respect to A_2 for ^{8}He fixed as a third particle.	47
4.7	Fragmentation potential plotted with respect to A_2 for ^{7}Be fixed as a third particle.	48
4.8	Fragmentation potential plotted with respect to A_2 for ^{8}Be fixed as a third particle	48

4.9	Fragmentation potential plotted with respect to A_2 for ^{9}Be fixed as a third particle.	49
4.10	Fragmentation potential plotted with respect to A_2 for ^{10}Be fixed as a third particle.	49
4.11	Fragmentation potential plotted with respect to A_2 for ^{11}Be fixed as a third particle.	50
4.12	Fragmentation potential plotted with respect to A_2 for ^{12}Be fixed as a third particle.	50
4.13	Fragmentation potential plotted with respect to A_2 for ^{13}Be fixed as a third particle.	51
4.14	Fragmentation potential plotted with respect to A_2 for ^{9}C fixed as a third particle.	51
4.15	Fragmentation potential plotted with respect to A_2 for ^{10}C fixed as a third particle.	52
4.16	Fragmentation potential plotted with respect to A_2 for ^{11}C fixed as a third particle.	52
4.17	Fragmentation potential plotted with respect to A_2 for ^{12}C fixed as a third particle.	53
4.18	Fragmentation potential plotted with respect to A_2 for ^{13}C fixed as a third particle.	53
4.19	Fragmentation potential plotted with respect to A_2 for ^{14}C fixed as a third particle.	54
4.20	Fragmentation potential plotted with respect to A_2 for ^{15}C fixed as a third particle.	54
4.21	Fragmentation potential plotted with respect to A_2 for ^{21}Mg fixed as a third particle.	55
4.22	Fragmentation potential plotted with respect to A_2 for ^{22}Mg fixed as a third particle.	55

4.23	Fragmentation potential plotted with respect to A_2 for ^{23}Mg fixed as a third particle.	56
4.24	Fragmentation potential plotted with respect to A_2 for ^{24}Mg fixed as a third particle.	56
4.25	Fragmentation potential plotted with respect to A_2 for ^{25}Mg fixed as a third particle.	57
4.26	Fragmentation potential plotted with respect to A_2 for ^{26}Mg fixed as a third particle.	57
4.27	Fragmentation potential plotted with respect to A_2 for ^{27}Mg fixed as a third particle.	58
4.28	Fragmentation potential for the ternary decay of ^{252}Cf with respect to A_2 for He isotopes fixed as a third particle.	59
4.29	Fragmentation potential for the ternary decay of ^{252}Cf with respect to A_2 for Be isotopes fixed as a third particle.	59
4.30	Fragmentation potential for the ternary decay of ^{252}Cf with respect to A_2 for C isotopes fixed as a third particle.	60
4.31	Fragmentation potential for the ternary decay of ^{252}Cf with respect to A_2 for Mg isotopes fixed as a third particle.	60
4.32	Fragmentation potential for the ternary decay of ^{252}Cf with respect to A_2 for ^{3}He, ^{10}Be, ^{14}C, Mg^{27} fixed as a third particle.	61

CHAPTER-I
INTRODUCTION

1.1 Introduction

Nuclear fission is a special type of nuclear reaction in which an excited compound nucleus breaks up generally into two fragments of comparable mass number. Fission usually occurs amongst the isotopes of the heaviest elements known, e.g., uranium, thorium etc., the two German Chemists Otto Hahn and F.Strassmann discovered nuclear fission in 1939. It happened to be one of the most important discoveries in Physics [1]. They made an unexpected discovery while they bombarded various elements with neutrons in the Kaiser Wilhelm institute of Chemistry in Berlin. They noticed that the majority of neutron–bombarded element changed only slightly during their experiment, but uranium nuclei changed greatly-almost as if the uranium nuclei were breaking into two more or less equal fragments [2]. Hahn and Strassmann found that when uranium was bombarded with slow neutrons, one of the reaction products is barium. Meitner and her nephew Otto Frisch, working in Sweden provided the correct explanation of Hahn and Strassmann results by suggesting that the uranium nucleus bombarded with neutron broke up into two large fragments. They gave the name nuclear fission to this new phenomenon. Since the atomic number of barium is 56, the other fragment produced in the fission of uranium should have the atomic number 36. It should thus be the nucleus of an isotope of krypton, which was subsequently identified. The two fragments produced in fission are known as fission fragments. The nuclear fission discovered by Hahn and Strassmann can be written as

$$^{235}_{92}U + {}^{1}_{0}n \rightarrow {}^{236}_{92}U^{*} \rightarrow {}^{141}_{56}Ba + {}^{92}_{36}Kr + \mathbf{3}\,{}^{1}_{0}n$$

They also postulated that about 200 million-electron volts (MeV) of energy will be released each time a uranium nucleus split (or fission) into approximately equal fragments [1].

1.2 Basic Fission Model

Bohr and wheeler gave the first theoretical treatment of the fission event based on the liquid drop model of nucleus in 1939. The liquid-drop model of the nucleus has been applied with some success to the problem of the nuclear fission. The theory gives a qualitative, and sometimes quantitative, picture of the process and has made possible the description of some of the properties of fission [3].

In this model the nucleus is assumed to behave as a liquid drop of an incompressible, electrically charged nuclear fluid which when not under the action of any external force, it adopts a spherical shape. The spherical shape of the liquid drop nucleus depends on a balance involving the surface tension forces and the coulomb repulsive forces. The stable nucleus splits into two fragments by undergoing series of changes as shown in figure 1.1. The nucleus combines with the incident neutron to form highly energetic compound nucleus. Its extra energy is partly the kinetic energy of the neutron but largely the added binding energy of the incident neutron. This energy appears to initiate a series of rapid oscillations in the drop, which tend to distort the spherical shape, so that the drop may become ellipsoidal in shape. The surface tension force tends to retain spherical shape, while the excitation energy tends to distort the shape still further. If the excitation energy is sufficiently larger, the drop may attain the shape of a dumb-bell. If the oscillation becomes so violent that stage fourth is inevitable.

Thus there is threshold energy or a critical energy required to produce stage fourth after which the nucleus cannot return to stage first. Finally the coulomb repulsive forces may then push the two “bells” apart until the dumbbell splits into two similar drops, each of which then becomes spherical in shape. If the excitation energy is not large enough, the ellipsoid may return to the spherical shape, with the excitation energy being liberated in the form of γ-rays and the process is one of radiation capture rather than fission [4].

1.3 Fission Process

The process of breaking up of the nucleus of a heavy atom into two, more or less equal fragments with the release of a large amount of energy is known as nuclear fission. In nuclear fission, the nucleus of a heavy element such as uranium or plutonium is bombarded by a neutron, which it absorbs. The resulting compound nucleus is unstable and soon breaks apart, or fission, forming two lighter nuclei called fission products and releasing additional neutrons [5].

1.4 Spontaneous Fission (SF)

Spontaneous fission has been defined as the process whereby a parent nucleus breaks into two daughter nuclei of approximately equal masses without any external action. The semi empirical mass formula (SEMF) predicts that the energy release is a maximum when the two fragments have exactly equal masses but experimentally precisely equal are found to be very unlikely.

Spontaneous fission is a potential barrier problem [6]. Figure 1.2 shows the potential energy (E) of the two fragments as a function of their separation of fragments (r). The figure 1.2 the curve is supposed to be divided into three regions. Considered the three regions, the process which would be the reverse of fission. In region (I) the fragments are completely separated and the two fragments mutually repel each other so that electrostatic coulomb energy is dominant.

In region (II) the drops just touch each other, at $r = 2R_0$ where R_0 is the radius of fragments. Potential energy (E) at that point is less than the corresponding coulomb potential by an amount CD. This amount is equal to the potential of the surface forces, which are just beginning to come into play at this point. As pass through region (II) critical distance r_c is reached. At $r = r_c$, the potential energy (E) curve has a maximum value E_b (E_b is barrier energy).

In region (III) the fragments have coalesced and the short-range nuclear forces are dominant. An additional amount of energy $E_a = E_b - E_f$, (E_f is fission energy) the activation energy is required by the nuclear system before the potential barrier can be surmounted and fission can take place. The activation energy (energy needed for spontaneous fission) determines the probability of spontaneous fission. For heavy nuclei, the activation energy is about 6MeV, but disappears for very heavy nuclei [7].

1.5 Induced Fission

Another possibility for fission is to supply the energy needed to overcome the barrier by a flow of neutrons. Because of the absence of a coulomb force, a neutron can get very close to the nucleus and be captured by the strong nuclear attraction. The parent nucleus may then be excited to a state above the fission barrier and therefore split-up. This process is an example of induced fission. Neutron captured by a nucleus with odd neutron number releases not just some binding energy, but also a pairing energy. This extra contribution makes a crucial difference to nuclear fission properties [6]. In the fission process energy released as the kinetic energy of the fragment and the released neutrons, as well as in the form of gamma radiation. Fission by fast neutrons the kinetic energies of the order of 1MeV are needed to fission most fissionable nuclei, and by slow neutrons the kinetic energies of the order of 0.1eV or less [8].

1.6 Fission Products

The investigation of the products of the fission of ^{235}U has shown that the range of mass number is from 72, probably an isotope of Zinc with atomic number 30 to 158, thought to be an isotope of europium with atomic number 63. About 97% of ^{235}U nuclei undergoing fission yield products which fall into two groups, a “light” group with mass numbers from 85 to 104 and a “heavy” group with mass numbers from 130 to 149 The most probable type of fission, which occurs in about 7% of the total, gives products with mass numbers 95 and 139. There are 87 possible mass numbers between 72 and 158, which may represent the total number of different nuclides formed as direct fission fragments.

If this were the case, the uranium nucleus should be capable of splitting, so that there are 30 different modes of fission, a different pair of nuclei being formed in each mode. The fission fragments have too many neutrons for stability and most of them decay by electron emission. Each fragment starts a short radioactive series, involving successive emission of electrons. These series are called “fission decay chains”, and each chain has three members, on the average, although longer and shorter chains frequently [9].

1.7 Mass distribution of fission products

The mass distribution of fission products can also be obtained from the distribution of their kinetic energies, which can be determined by measuring the ionization produced in an appropriate ionization chamber. In one type of chamber, the fissile material is placed on one of the electrodes and the ions which result when a fission fragment enters the region between the electrodes are collected, since the fission fragments occur in pairs, an experiment of this kind measures the energy of one fragment only. In another type of chamber, a very thin foil is made the common cathode of two fragments resulting from neutron bombardment travel in opposite direction into the two chambers and the ionizations they cause are measured simultaneously.

The nucleus undergoing fission can be considered to be initially at rest; and, if the neutrons emitted are neglected, the law of conservation of momentum gives

$$M_1V_1=M_2V_2$$

where subscripts refer to the two fission fragments. The energies of the fragments are

then in the ratio $$\frac{E_1}{E_2}=\frac{\frac{1}{2}\left(M_1V_1^{\,2}\right)}{\frac{1}{2}\left(M_2V_2^{\,2}\right)}=\frac{M_2}{M_1}$$ ---------- (1.1)

The masses are inversely proportional to the kinetic energies; when the energy distribution has been measured, the mass distribution is obtained from equation (1).
The energy distribution of the fragments from spontaneous fission has also been determined and is similar to that found in neutron-induced fission. Mass distribution of the fission process is highly asymmetric for thermal neutron bombardment; symmetric mass distribution occurs in only 0.001% of the cases. There are also small, fine structure peaks, which probably results from the shell effect that favors the formation of certain mass pairs as compared to other neighboring mass pairs.

.

1.8 Energy and charge distribution of fission products

The energy distribution of the fission products has been measured for the fission of ^{233}U, ^{238}U and ^{239}Pu by thermal neutrons, and for the fission of ^{235}U, ^{238}U, ^{232}Th and ^{239}Pu by fast neutrons. The kinetic energy distribution of fission fragments

of ^{235}U bombarded by thermal neutrons. When the two fragments of fission are formed, they are in highly excited states, which de-excite by the emission of neutrons, γ-rays or conversion electrons. The curve corresponding to all γ-rays represents the normal distribution of kinetic energies of the fragments, however if the kinetic energy distribution is studied as the function of the energy of γ-rays. The conclusion from that is higher-energy γ-rays are preferentially emitted for symmetric fission and by doubly magic number nuclei such as N=82 and Z=50 [9].

The determination of the charge distribution in fission is more difficult than that of the energy distribution because in an ionization chamber or cloud chamber there is no obvious way of determining the nuclear charge at the instant of fission [9].

1.9 Binary Fission

Binary fission induced by high-energy particles is defined as the decay of the nucleus into two fragments of comparable masses with an angle between their emission directions larger than 90° [10].

1.10 Ternary Fission (TF)

Fission is a process in which only two particles (fission products) are formed. If three particles are formed in the fission process, we have a ternary fission. Ternary fission was found for spontaneous fission, as well as in induced fission. In ternary fission process, with three charged particles in the outgoing channel, the third particle being very light compared to the main fission fragments situated between these two extremes, is called light charged particle (LCP) accompanied fission [11]. Light charged particle- (LCP) accompanied fission, (ternary fission) is a rare process relative to binary fission The most observed LCP (about 90%) accompanying ternary fission is the α particle, preferentially emitted in a direction orthogonal to the fission axis. The probability of ternary fission relative to binary fission is small, $P_t/P_b \sim 10^{-3}$ where P_t is fission probability and P_b is binary fission probability. The dependence of LCP yield on excitation energy is very weak and in two known cases it decreases at transition from spontaneous fission to induced fission. The very sharp LCP charge and mass distribution: almost all particles emitted are alpha particles. The latter feature is connected not only with the mechanism of LCP formation but also with the effects of nucleon exchange in ternary nuclear system [12]. The angular distribution of

these LCPs accompanying the ternary fission reveals that they are formed in the neck region between the two main fission fragments and emitted in a direction perpendicular to the fission axis as a result of high Coulombic force. The ternary fission process in which the third fragment is emitted in a direction perpendicular to the fission axis, is termed as equatorial or orthogonal emission as shown in figure. 1(a) and if the third fragment is emitted in the direction of fission axis along with the other two fragments is termed as collinear or polar emission as shown in figure. 1(b) [13].

1.21 Mechanism of Ternary Fission

Several approaches have been suggested to explain the mechanism of this ternary fission. There are three main groups of ternary fission mechanism explanations.

- ✓ The statistical models.
- ✓ The formation of light charged particles (LCP) in the fission was treated, as α-decay.
- ✓ The formation of LCP is treated as dynamic process of light nucleus creation at the moment of neck scission.

In TF, nucleons from the neck formed between the main fragments right at scission cluster into a light third nucleus that is ejected at about right angle to the fission axis, due to the focusing by the Coulomb field from the nascent fragments.

The formation of LCP species in ^{235}U and ^{252}Cf (SF) that are unstable against neutron decay from their ground states was discovered already some 30 years ago in coincidence experiments between ternary α particles and neutrons. It is worthwhile to note that ternary fission with the emission of neutron-unstable. LCP provides a source of neutrons that are emitted at about right angles to the fission axis [14].

.

1.22 Cold and Hot Ternary Fission

The cold ternary fission is a rearrangement process of a large group of nucleons from the ground state of the initial nucleus to the ground state of the three final fragments. Like in the case of spontaneous and thermal-induced fission a ternary component of a few tenths of percent is present also in the cold fission process

[15,16,17]. The main characteristic of cold nuclear fragmentations is the emission of final nuclei with very low or even zero excitation energy and with high kinetic energies pointing thus to rather compact shapes of the fragments for the scission configuration. The fact that the light charged particles (LCP) emitted in ternary fission (including the cold splittings) are focused mainly into the equatorial plane perpendicular to the fission axis seems to indicate that most of the ternary clusters originate from the region of the neck between the two heavier fragments [18]. It is very important to establish theoretically and experimentally if cold (neutronless) ternary fragmentations similar to the cold binary ones exist in nature. This new phenomenon will be equivalent to cluster radioactivity during the fission. Such cold ternary decays will produce all three fragments with very low or even zero internal excitation energy and consequently with very high kinetic energies. Their total kinetic energy TKE = Q_t − TXE where TXE stands for the total excitation energy, will be close to the corresponding ternary decay energy Q_t. In order to achieve such large TKE values, the three final fragments should have very compact shapes at the scission point and deformations close to those of their ground states, similar to the case of cold binary fragmentations [19,20].

In the binary nuclear fission of actinide nuclei the fragments are usually formed in highly excited states that subsequently decay to their ground states by emitting neutrons and γ rays. However a small fraction of these fragmentations will attain a very high kinetic energy *TKE* that is very close to the corresponding binary decay energy *Q*. Since in this case the fragments are formed with excitation energies close to their ground states no neutrons are emitted. Milton and Fraser [21] noticed that some of the fission fragments are produced at such high kinetic energies that the emerging nuclei are formed nearly in their ground state. Later on Guet *et al.* [22] confirmed the previous interpretation by determining the mass distributions of the primary fragments for the highest values of the kinetic energy. They concluded that even before the scission takes place we deal with a superposition, of two fragments in their ground state, from which the cold fragmentation term emerged. An interesting remark they made was that the odd-even fluctuations of *Q* due to nucleon pairing were not present also in the TKE_{max} values. In their view this smoothing of the odd-even effect was a consequence of a pair broken from one of the fragments. The cold (neutronless) fission of many actinide nuclei into fragments with masses ranging from ~70 to ~160 has been clearly observed [23–28]. An extreme case is the bimodal

fission observed for the Fm and Md isotopes [29] where two distinct fission channels were observed, one with very high total kinetic energy (TKE) corresponding to the cold fission with compact scission shape fragments and the second one at much lower TKE's with elongated fragments at scission. All these observations confirmed the theoretical predictions regarding the cold rearrangement processes of large groups of nucleons from the ground state of an initial nucleus to the ground states of the two final fragments [30,31]. The process in which a heavy nuclei splits along with the evaporation of neutron is called hot fission [32-33]. However, the energy cost for emitting ternary particles is so high that standard statistical evaporation can be ruled out. This has led many authors to conclude that ternary fission is a dynamical process not associated with an evaporative process.

1.23 Models of Ternary Fission

Usually the third light particles carry information about the fission process. In order to extract this information from the experimental data one needs a model relating the assumptions for the (not directly observable) fission process with the observed emission probability and with the angular and energy distributions. The most widely used models are classical trajectory calculations. These models start with some initial distribution for the location and velocity of α-particle. The α-particle moves in the average potential of the fissioning nucleus. Due to the time dependence of the potential some α-particles gain enough energy to overcome the Coulomb barrier. These α-particles are their emitted.

In the classical models one finds that the predominant emission in the direction perpendicular to the fission axis is due to α-particles from the neck region. The main disadvantage of the classical models is (besides the classical treatment itself) the arbitrariness of the distribution of initial conditions. Extensive trajectory calculations have shown that rather different sets of initial conditions may lead to similar energy and angle distributions.

In quantum mechanical model it is started with a quasi-bound α-particle wave function in the initial nucleus (before the fission process sets in). As in the classical model, this α-particle is assumed to move in the average potential of the fissioning nucleus. This motion is treated quantum mechanically, i.e. the time-dependent Schrodinger equation for the α-particle is solved. For α-particles that have surpassed

the Coulomb barrier the motion is continued classically. The energy gain of the α-particle due to the time dependence of the potential (which is the decisive part of the process) is treated quantum mechanically. Disadvantage of this model is that in order to get the energy and angular distribution of the α-particle the wave function must be eventually connected to classical trajectories; this involves some ambiguity [34].

1.24 Cluster and Ternary Fission

Cluster decay is a radioactive decay in which the emitted particle is heavier than alpha. Cluster radioactivity or heavy ion radioactivity is an intermediate process between alpha decay and nuclear fission. In this process, cluster heavier than alpha particles but lighter than fission fragments are produced. The first cluster decay was obtained in 1984 [35] and the emitted particle was ^{14}C. Rose and Jones realized that cluster radioactivity will lead to a nucleus of high stability, usually to a magic or double magic nucleus. However, during this decay process, not only the stability of the resultant nucleus is important, but also of the cluster itself. The most important clusters in cluster decay are: ^{14}C among the carbon isotopes, ^{20}O among the oxygen isotopes, ^{24}Ne among the neon isotopes, ^{28}Mg among magnesium isotopes, and for the silicon isotopes, it is either ^{34}Si or ^{32}Si. The most common mode of fission is division into two fragments of roughly equal masses; in about one event in a few hundreds a third light charged particle is emitted. This phenomenon is often given the name ternary fission, although the same name is also sometimes used for the much rare division into three more or less equal fragments [36]. Overall 90% of the light, charged particles emitted in ternary fission are alpha particles [37-39] and hence, the terms “ternary fission” and “fission with long-range alpha particles are frequently interchangeably.

The ternary fission products that have the highest yields are:

^{3}H among the hydrogen isotopes.

^{6}He among the helium isotopes, if ^{4}He is considered as a class by itself.

^{11}B among the boron isotopes, although with a relatively low yield, compared to ^{10}Be.

^{14}C among the carbon isotopes.

^{20}O among the oxygen isotopes.

^{22}F among the fluorine isotopes, although with a relatively low yield, compared to ^{20}O.

^{24}Ne among the neon isotopes, although with a relatively low yield.

^{28}Mg among the magnesium isotopes.

The yields for the different silicon isotopes are of the same order of magnitude. So the most important ternary particles, in respect to their yield, are: ^{3}H, ^{4}He (^{6}He), ^{10}Be, ^{14}C, ^{20}O, ^{24}Ne and ^{28}Mg. Although the high yield of these clusters was obtained in ^{a} ^{241}Pu reaction, similar results may also be obtained from ^{233}U , ^{235}U, ^{239}P and ^{242}Am [15]. Besides the light particles, ^{3}H and ^{10}Be, these ternary particles are the same as the clusters obtained in cluster decay. This similarity suggests that cluster decay and ternary fission are related. The similarity between ternary fission and cluster decay suggests that just as ternary alpha emission may be seen as alpha decay, other ternary emissions can be considered to be cluster decays. Like the interpretation given by [40], they would like to suggest that ternary fission is a cluster decay of the fissioning nucleus in the last phase of the scission process. They have also suggested that the clusters obtained in cluster radioactivity, as well as the clusters with high yield obtained in ternary fission, are also related among themselves, at least for the light clusters.

1.15 Objectives of the study

Aim of this study is to calculate the fragmentation potential by fixing the third particle for the parent nuclei ^{252}Cf in ternary fission. This includes the calculation of coulomb potential, proximity potential and binding energy for the three fragments.

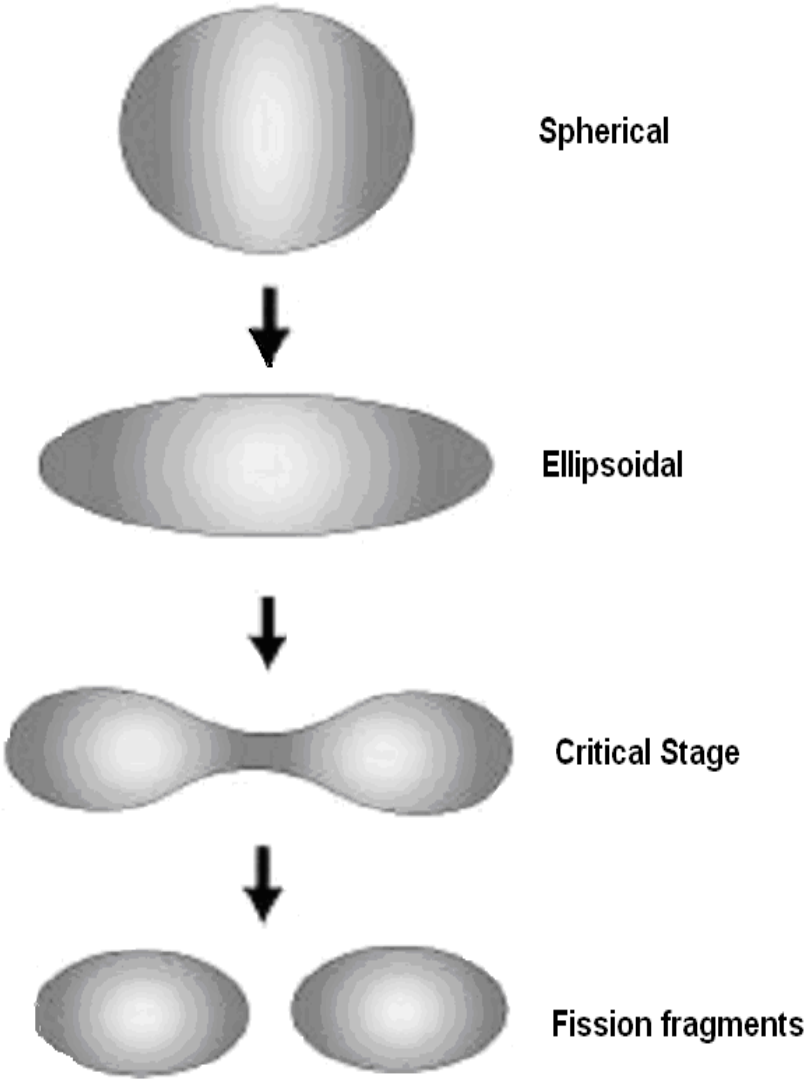

Figure 1.1 Steps in the process of nuclear fission according to the liquid drop model.

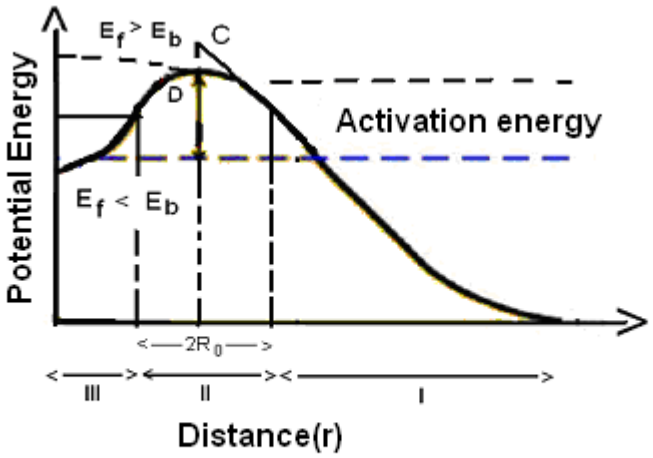

Figure 1.2 Potential energy during different stages of a fission.

(a) Equatorial

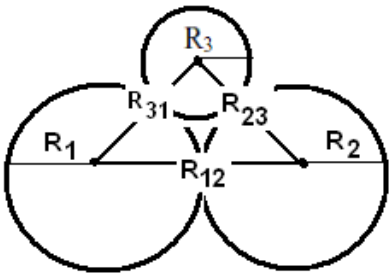

(b) Collinear

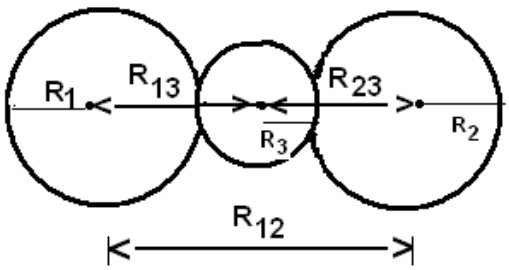

Figure 1.3 Schematic touching configurations of the spherical nuclei in Ternary Fission.

Reference:

[1]. S.N. Ghoshal, Atomic and Nuclear Physics, S.Chand & company Ltd, **2,** 670 (2000).

[2]. Joseph A. Angelo, Jr, Nuclear Technology, Greenwood publication, 19, (2004).

[3]. K.Samson, Nuclear Physics, Sarup & Sons, 221, (2003).

[4]. M.L. Pandya, R.P.S. Yadav, Kedar Nath Ram Nath Publication, Elements of Nuclear Physics, 490, (2007).

[5]. B.R. Martin, Nuclear and particle Physics, A John Wiley and Sons Ltd, 59, 62, (2009).

[6]. Arthur Beiser, Concepts of modern Physics, Tata McGraw-Hill Publishing Company LTD, **6,** 450, (2008).

[7]. D.C. Tayal, Himalaya Publishing House, Nuclear Physics, 531, (2007).

[8]. A.K. Saxena, Narosa Publishing House, Principles Of Modern Physics, **2**, 13.9, (2007).

[9]. Irving Kaplan, Nuclear Physics, Narosa Publication, 615, 617, (1998).

[10]. Z. Todorovic, R. Antanasijevic, and M. Juric, Z. Physik, **266**, 29 (1974).

[11]. Y. Ronen, Annals of Nuclear Energy **29**, 1013 (2002).

[12]. I.Halpern, Ann.Rev.Nucl.Sic **45,** 21 (1971)**.**

[13]. K. Manimaran and M. Balasubramaniam, Phys.Rev C **83**,034609 (2011).

[14]. V.A. Rubchenya and S.G. Yavshits, Z. Phys. A - Atomic Nuclei **329**, 217 (1988).

[15]. C.Wagemans, The Nuclear Fission Process, CRC Boca Raton FL, (1991).

[16]. F.Goennenwein et al., 6-th Int.Conf. On Nuclei Far from Stability and 9-th Int.Conf. On Atomic Masses and Fundamental Constants, Bernkastel-Kue 453, (1989).

[17]. A.V.Ramayya et al., Phys.Rev. C **57**, 5 (1998).

[18]. A. Florescu, A. Sandulescu, D. S. Delion, J. H. Hamilton, A. V. Ramayya, and W. Greiner. Phys. Rev C, **61**, 051602(R) (2000).

[19]. A. Sandulescu, A. Florescu and W. Greiner, J. Phys. G: Nucl. Part.Phys. **15**, 1815, (1989).

[20]. F. Gonnenwein and B. Borsig, Nucl. Phys**. A530**, 27 (1991).

[21]. J.C.D. Milton and J.S. Fraser, Can. J. Phys. **40**, 1626 (1962).

[22]. C. Guet, M. Ashgar, P. Perrin, and C. Signarbieux, Nucl. Instrum. Methods **150**, 189 (1978).

[23]. F.J. Hambsch, H.-H. Knitter, and C. Budtz-Jorgensen, Nucl.Phys. **A554**, 209 (1993).

[24]. A. Benoufella, G. Barreau, M. Asghar, P. Audouard, F.Brisard, T. P. Doan, M. Hussonnois, B. Leroux, J. Trochon, and M. S. Moore, Nucl. Phys. **A565**, 563 (1993).

[25]. W. Schwab, H.-G. Clerc, M. Mutterer, J. P. Theobald, and H.Faust, Nucl. Phys. **A577**, 674 (1994).

[26]. J. H. Hamilton, A. V. Ramayya, J. Kormicki, D. Shi, J. K. Deng, et al., J.Phys. G **20**, L85 (1994).

[27]. G. M. Ter-Akopian, J. H. Hamilton, Yu. Ts. Oganessian, J.Kormicki, G. S. Popeko, A. V. Daniel, et al., Phys. Rev. Lett. **73**, 1477 (1994).

[28]. A. Sandulescu, A. Florescu, F. Carstoiu, W. Greiner, J. H.Hamilton, A. V. Ramayya and B. R. S. Babu, Phys. Rev. C **54**, 258 (1996).

[29]. E. R. Hulet, J. F. Wild, R. J. Dougan, R. W. Lougheed, J. H.Landrum, et al., Phys. Rev. Lett. **56**, 313 (1986).

[30]. A. Sandulescu and W. Greiner, J. Phys. G **3**, L189 (1977).

[31]. A. Sandulescu, J. Phys. G **15**, 529 (1989).

[32]. D. J. Hinde *et al.*, Nucl. Phys. **A 452**, 452 (1986).

[33]. J. P. Lestone *et al.*, Nucl. Phys. **A 559**, 277 (1993).

[34]. J P. Theobald, P. Heeg and M. Mutterer, Nucl. *Phys.* A ***502,*** 343 (1989).

[35]. H.J. Rose and G.A.Jones, Nuture **307**, 245 (1984).

[36]. E.K. Hyde, The Nuclear Properties of the Heavy Elements **3**, 131 (1964).

[37]. C.B. Fulmer and B.L. Cohen, Phys.Rev. **108,** 370 (1957).

[38]. H.E.Wegner, Bull. Am. Phys. Soc. **6,** 307 (1961).

[39]. T.C. Watson, Phys. Rev. **121**, 230 (1961).

[40]. N. Carjan, Surlorigine des alphas de scission. J. Phys. **37**, 1279 (1976).

CHAPTER-II
REVIEW OF LITERATURE

2.1 Introduction

Nuclear fission is defined as the breakup of heavy nuclei into two fragments. These fragments attain about 90% of their kinetic energy within a time interval of several times 10^{-20}s. Within the same time interval, there is also a probability of three particles being formed. Theoretically, fission with the formation of three particles is called ternary fission i.e., includes the formation of a third particle, with masses ranging from scission neutrons to middle-heavy fragments when a compound nucleus splits into three parts of comparable mass. Leaving aside the scission neutrons, about 90% of ternary particles are alpha particles; about 7% are tritons and the rest are heavier nuclei [1]. Since the yield of the lightest ternary particles is comparable to that of binary fragments of given mass and charge, detailed studies could already be performed in 1960s and 1970s [2–6]. It was observed that most of the ternary alpha's are emitted perpendicularly to the fission axis, and only a small fraction (about 3%) are emitted from accelerated fragments (i.e., along the fission axis) [7]. As in binary fission, odd-even effects in the yields of light ternary particles were found; particles with even proton and neutron numbers (such as ^{4}He, ^{10}Be, and ^{14}C) appear more frequently in ternary fission than those with odd *Z* and N number [1].

2.2 Review on theoretical studies on ternary fission of ^{252}Cf

Ismail *et al.*, (2013) studied the ternary fission of the $^{238-256}$Cf even-A isotopes in the framework of the three-cluster model within the spherical approximation. The study is confined to those decays in which the accompanied light charged particle is of mass A=10. The most probable ternary fission path is obtained as the one that has a peak in the Q-value and a minimum for the driving potential, with respect to the mass and charge asymmetries. Assuming both equatorial and collinear configurations of the different emissions of light charged particles with A=10, the ternary fission of ^{252}Cf is found to be most favored with ^{10}Be. The predicted favorable fragmentation channels of the ^{10}Be accompanied ternary fission of $^{238-256}$Cf, even-A, isotopes are

discussed in detail. The closed shell structure of the produced heaviest fragment is found to play the key role for the detected most favorable channels. A nucleus with closed neutron shell or even doubly closed shell is always appearing as the heaviest nucleus in the favored channel of the ternary fission of all mentioned isotopes. As the isospin asymmetry of the isotope increases the width of its cold fission valley around the symmetric mass region decreases, with more shifting towards the centre of the symmetric region. The most favorable ternary emissions and the behavior of the ternary fragmentation potential did not change with the change of the type of the nuclear interaction potential (Yukawa, folding potential with Migdal force and proximity 77). Also, almost no change is observed according to the method of emission of the fragments (equatorially or collinearly) or when the calculations are performed without inserting the nuclear interaction potential.

Vijayaraghavan *et al.*, (2012) calculated the kinetic energy distribution and potential energies of fragments from the collinear cluster tripartition (CCT), the "true" ternary fission of ^{252}Cf. It is assumed that the breakup of the nucleus into three fragments happens sequentially in two steps from a hyper-deformed shape. In the first step a first neck rupture occurs of the parent radioactive nucleus, forming two fragments (one of them is usually ^{132}Sn) and, in the second step, one of the two fragments breaks into two other fragments, resulting finally in three fragments (the experiment is based on a binary coincidence where a missing mass is determined). They showed the result for the principal combination of the three spherical fragments (semi-magic isotopes of Sn, Ca, Ni) observed recently experimentally. These isotopes are clusters with high Q -values, which produce the highest yields in the ternary fission bump. It is shown that the kinetic energies of the middle fragments have very low values, making their experimental detection quite difficult. This fact explains why the direct detection of true ternary fission with three fragments heavier than $A > 40$ have escaped experimental observation.

Mirzaei *et al.*, (2012) investigated a nuclear shape parameterization that leads to the formation of three collinear fragments of the ternary fission. The deformation energy was computed within the liquid drop model in the framework of the Yukawa-plus-exponential mode. The ternary fission barrier was estimated by taking into

account deformation dependent terms as the volume energy, the Coulomb energy, and the surface energy. The trajectory after the scission of the ternary system was computed by solving twelve differential motion equations related to the motion. Finally the penetrability for binary and ternary processes was compared.

Manimaran and Balasubramaniam (2011) studied all possible ternary fragmentations in fission of ^{252}Cf in collinear configuration within a spherical approximation using the recently proposed "three cluster model." The potential energy surface of collinear configuration exhibits a strong valley around ^{48}Ca and its neighboring nuclei ^{50}Ca, ^{54}Ti, and ^{60}Cr. Such strong minima are not seen in the potential energy surface of an equatorial configuration. As a consequence of strong minima in the potential, the overall relative yield is higher for the ternary fragmentation with ^{48}Ca, ^{50}Ca, ^{54}Ti, ^{60}Cr, and ^{82}Ge as the third fragment. The results of potential energy and relative yield calculations reveal that collinear configuration increases the probability of emission of heavy fragments like ^{48}Ca (doubly magic nucleus) and its neighboring nuclei as the third fragment. The obtained results indicate that the collinear configuration is the preferred configuration for intermediate nuclei (^{48}Ca, ^{50}Ca, ^{54}Ti, and ^{60}Cr) as the third fragment in particle accompanied fission while the equatorial configuration may be a preferred configuration for light nuclei (^{4}He, ^{10}Be) as the third fragment.

Manimaran and Balasubramaniam (2010) studied the ternary fragmentation by calculating the potential energy surfaces (PES) with the inclusion of deformation and orientation degrees of freedom for the ^{4}He- and ^{10}Be-accompanied fission of the ^{252}Cf nucleus. The most favored ternary fragmentation channels in the light charged particles (^{4}He and/or ^{10}Be)-accompanied fission of the ^{252}Cf nucleus are predicted using the PES calculations. The sensitivity of PES due to the ground state quadrupole deformation (β2) and the orientation effects (90°–90° and 0°–0°) of the fragments are analyzed.

Manimaran and Balasubramaniam (2010) investigated the ternary fragmentation of ^{252}Cf for all possible third fragments using the recently proposed

three-cluster model within a spherical approximation and satisfying the condition $A_1 \geq A_2 \geq A_3$. The most probable ternary configurations in the fission of ^{252}Cf accompanied with all possible third fragment mass numbers from A_3 = 1 to 84 are predicted and their independent and overall relative yields are calculated. The calculations of the properly charge minimized potential energy surface (PES) and yield reveal that even-mass third fragments are more favored than odd ones. In the most probable configuration having the minimum in the potential energy and the maximum in yield, among the three fragments, at least one (or two) of the fragment(s) associates itself with the neutron (or proton) closed shell and in some cases even with the doubly closed shell. The calculated relative yields imply that next to ^{14}C (the heaviest third fragment observed in the spontaneous ternary fission of ^{252}Cf , $^{34, 36, 38}$Si , $^{46, 48}$Ar , and $^{48, 50}$Ca are presenting themselves as the most favoured cases to be observed as the third particle in the spontaneous ternary fission of ^{252}Cf .

Manimaran and Balasubramaniam (2009) developed a three-cluster model, to explain the particle-accompanied binary fission of radioactive nuclei. The model is developed as an extension of the preformed cluster model of Gupta and collaborators. The advantage of this model is that, for a fixed third fragment, they can calculate the fragmentation potential minimized in charge coordinate. For their study they chose the various neutron-deficient to neutron-rich californium nuclei, whose analysis reveals that the closed-shell effect of any one of the fragments in ternary fragmentation presents itself as the most favorable configuration. As one goes from a neutron-deficient to a neutron-rich californium isotope, the role of the neutron closed shell associated with any one of the preferred fragments changes to that of the proton closed shell, and for very neutron rich isotopes of californium the presence of a double closed shell nucleus enhances the decay probability. The quadrupole deformation of the light fragment (A_2) associated with the preferred configuration in the symmetric mass region also has a transition from positive to negative deformation as one goes from neutron-deficient to neutron-rich californium isotopes**.** The calculated relative yields of different fragmentation channels are compared with the available experimental yields for ^{252}Cf.

Lestone *et al.*, (2005) calculated the yields of hydrogen, helium, lithium, and beryllium isotopes. In thermal neutron-induced and spontaneous fission the addition

of two neutrons to a neutron-even system produces only minor changes to the shape, kinetic energy, and temperature of the scission configuration. If these changes are assumed negligible and if ternary fission is associated with a statistical process then the ratio of ternary fission yields for systems differing by two atomic mass units can be used to infer a nuclear temperature. Yields of hydrogen, helium, lithium, and beryllium isotopes ejected perpendicular to the direction of the main fragments from ^{233,235}U,^{239,241}Pu, and ^{250,252}Cf spontaneous fission give a nuclear temperature T=1.24±0.10 MeV. The yield of polar α particles from ^{233,235}U give T=1.13±0.24 MeV. These results are in agreement with other inferred low-energy ternary fission temperatures and support the idea that both equatorial and polar ternary fission involve a statistical process where the ejected particles are in equilibrium with a heat bath with a temperature slightly hotter than 1 MeV.

Wagemans *et al.*, (2004) studied the good experimental conditions for the ^{235}U ternary α energy distribution at the reactor of the ILL in Grenoble. An intense and clean neutron beam, a small, thin sample of highly enriched U could be used, with an activity of only 1.6 Bq, so the measurements could be done without absorber in between the sample and the ΔE–E detector. With the resulting low detection limit of 6 MeV, a clearly asymmetric energy distribution was obtained, deviating by 6% from a Gaussian shape. This energy distribution has been deconvoluted into components corresponding to "true" ternary α's and α's originating from the decay of ^{5}He particles. Ternary α emission yield data have been re-evaluated accordingly.

Mutterer and Kopatch (2003) studied the rare ternary fission (TF) process mainly by inclusive measurements of the energies and fractional yields of the light charged particles (LCPs) from fission, or by experiments on the angular and energy correlation between LCPs and fission fragments (FF). The present article briefly describes a series of recent correlation measurements on ^{252}Cf (SF) TF that include either the registration of neutrons and γ rays with LCPs and FFs, or the coincident registration of two LCPs. The population of excited states in LCPs has been identified, as well as the formation of neutron-unstable nuclei as short-lived intermediated LCPs, the sequential decay of particle-unstable LCP species into charged particle pairs, and "quaternary" fission with the emission of two charged particles right at scission.

Kopatch *et al.*, (2002) measured the neutron-unstable odd-N isotopes ^{5}He,^{7}He and ^{8}Li (in its excited state of E^{*} = 2.26 MeV) to show up as short-lived(τ approximately equal to 10^{-21}-10^{-20} s) intermediate light charged particles (LCPs) in ternary fission of ^{252}Cf. For the study a high-efficiency angular correlation measurement between neutrons, LCPs, and main fission fragments has been performed. The evidence for the ternary ^{5}He and ^{7}He particles (lifetimes: 1×10^{-21} s, and 4×10^{-21} s, respectively) was disclosed from the measured angular distributions of their decay neutrons focused by the emission in flight towards the direction of motion of ^{4}He and ^{6}He ternary particles. Similarly, neutrons observed to be peaked around Li-particle motion could be attributed to the decay of the second excited state at E^{*}=2.26 MeV (lifetime: 2×10^{-20} s) of ^{8}Li. The fractional yields of the intermediate ^{5}He and ^{7}He ternary fission modes relative to the "true" ternary ^{4}He and ^{6}He modes, respectively, were determined to be 0.21(5) for both cases. The mean energy of the ^{4}He residues resulting from the ^{5}He decay was determined to be 12.4(3) MeV, compared to 15.7(2) MeV for all ternary α particles registered, and to 16.4(3) MeV for the true ternary α particles. The mean energy of the ^{6}He residues from the ^{7}He decay is 11.0(15) MeV, compared to 12.3(5) MeV for all ternary ^{6}He particles. The population of ^{8}Li* was deduced to be 0.06(2) relative to Li ternary fission, and 0.33(20) relative to the yield of particle stable ^{8}Li. The perspective of using the observed intermediate LCPs for probing the ternary scission configuration in ^{252}Cf fission with the aid of trajectory calculations is briefly discussed.

Manfred Mutterer (2001) observed the particle-accompanied fission, known also as ternary fission, is a process where, close to the instant of scission, a light charged particle is ejected from the space between the emerging fission fragments. Since only a few fission events in a thousand are such ternary fragmentations, precise ternary fission experiments are generally hard to perform. The study is primarily concerned with a recent experimental study on the ternary fission of ^{252}*Cf* (*SF)* which was carried out with the Darmstadt-Heidelberg 4π *NaI*(*Tl*) Crystal Ball spectrometer as highly efficient γ-ray and neutron detector which was additionally equipped with detectors for fission fragments and ternary particles. This advanced multiparameter study was able to cover besides the most abundant (α-particle-accompanied fission process also much rarer fission modes with emission of various ternary particles, from tritons to carbon nuclei.

Delion *et al.*, (2001) studied the dynamics of light charged particle emission in the cold fission of ^{252}Cf in terms of spheroidal coordinates. This system of coordinates provides a more adequate description for a hyperdeformed fissioning nucleus than the standard spherical variables. They derive the system of coupled differential equations describing the motion of the emitted light cluster and they give a generalization of the Fröman matrix. The phase-shift analysis predicts long half-lives with respect to the characteristic particle nuclear time, but shorter than the cold fission transient time for those fissioning configurations that are emitting α particles and ^{10}Be. Consequently, such configurations could be interpreted as ternary nuclear molecules.

Misicu *et al.*, (2000) proposed a model to calculate the shift of the vibrational 2_1^+ state in ^{10}Be when its heavy companions are the even-even nuclei ^{146}Ba and ^{96}Sr. The stiffness parameters of the β vibrations are calculated within the self-consistent Hartree-Fock method with BCS pairing correlations taken into account, and their change is determined by the interaction of the light cluster with the heavy fragments. The results point to a dependence of the shift magnitude and signature on the relative distance between the three clusters and their mutual orientation. Eventually it is the anharmonic perturbation of the spherical vibrator, which is responsible for obtaining a negative energy shift of the 2_1^+ state.

Carstoiu *et al.*, (2000) used a coplanar three-body cluster model (two deformed fragments and a α particle) with a three-body potential computed by a double folding potential generated by M3Y effective interaction. A repulsive compression term was included. The computed α ternary cold fission yields are in agreement with the experiment. The energy and angular distributions of the three clusters at infinity and the half-lives are strongly dependent of the initial positions of the α particle relative to the two fragments and of mass asymmetry of the fragments. The evaluated lifetimes of such trinuclear molecules are quite large, of the order of one second.

Hwang *et al.*, (2000) determined the relative ^{4}He and ^{5}He ternary fission yields from a careful analysis of the energy distribution of α spectra from a new measurement with a ^{252}Cf source and from published data on ^{252}Cf and ^{235}U. The kinetic energies of the ^{5}He and ^{4}He ternary particles were found to be approximately

11 and 16 MeV, respectively. ^{5}He particles contribute 10–20 % to the total alpha yield with the remainder originating from ^{4}He accompanied fission.

Sandulescu *et al.*, (1999) observed a coplanar three body cluster model (two deformed fragments and an α particle), similar to the model used for the description of cold binary fission, was employed for the description of cold (neutronless) α accompanied fission of ^{252}Cf. No preformation factors were considered. The three-body potential was computed with the help of a double folding potential generated by the M3Y-NN effective interaction and realistic fragment ground state deformations. From the minimum action principle, the α particle trajectory equations, the corresponding ternary barriers, and an approximate WKB expression for the barrier penetrability are obtained. The relative cold ternary yields were calculated as the ratio of the penetrability of a given ternary fragmentation and the sum of the penetrabilities of all possible cold ternary fragmentations. Different scenarios were considered depending on the trajectories of the fragments. It was shown that two regions of cold fragmentation exist, a deformed one corresponding to large fragment deformations and a spherical one around ^{132}Sn, similarly to the case of the cold binary fission of ^{252}Cf. They shown that for the scenario corresponding to the Lagrange point, where all forces acting on the α particle are in equilibrium, the cold α ternary yields of ^{252}Cf are strongly correlated with the cold binary yields of the daughter nucleus ^{248}Cm into the same heavy fragments. For all other scenarios only the spherical splittings are favored. They concluded that due to the presently available experimental data on cold α ternary yields only the Lagrange scenario could describe the cold α ternary fission of ^{252}Cf.

Poenaru *et al.*, (1999) made a comparison between observed ^{252}Cf cold binary fission, and cold ternary (accompanied by α particle or by ^{10}Be cluster). In this process a heavy or superheavy nucleus spontaneously breaks into four, five, or six nuclei of which two are asymmetric or symmetric heavy fragments and the others are light clusters, e.g., α particles, ^{10}Be, ^{14}C, ^{20}O, or combinations of them. Examples are presented for the two-, three-, and four-cluster accompanied cold fission of ^{252}Cf and ^{262}Rf, in which the emitted clusters are 2α, α+^{6}He, α+^{10}Be, α+^{14}C, 3α, α+^{6}He+^{10}Be, 2α+^{6}He, 2α+^{8}Be, 2α+^{14}C, and 4α. The strong shell effect corresponding to the doubly magic heavy fragment ^{132}Sn is emphasized. The most favorable mechanism of such a

decay mode should be the emission from an elongated neck formed between the two heavy fragments.

Florescu *et al.*, (1999) observed cold (neutronless) α-and^{10}Be-accompanied fragmentation of ^{252} Cf by triple γ coincidence technique with Gammasphere with 72 detectors. New experiments on ternary fission of ^{252} Cf are made now with Gammasphere at Argonne National Laboratory. An improved microscopic theory of cold ternary fragmentations has to include preformation probabilities of the light charged particles (LCP). They obtain the preformation amplitudes for such LCP (e.g. ^{4} He, ^{6} He, ^{10} Be and ^{14}C) within a microscopic approach starting from realistic single particle Woods-Saxon wave functions and employing a large space BCS-type configuration mixing. A pairing interaction is acting among neutrons and separately among protons. In order to calculate the preformation probability, they integrate separately over the coordinates of the two heavier final fragments taken as a core, then transform the individual coordinates of the nucleons forming the LCP into their relative (Jacobi) coordinates and further integrate on the LCP internal coordinates. The LCP internal functions are obtained with the usual ansatz prescribed by cluster-type nuclear structure theories. The chosen cluster oscillator constants α_{cl} reproduce the experimental nuclear radii. The highest cluster preformation probabilities are obtained for the neck region between the two heavier fragments. As the two heavier fragments move away from their touching point, the position of the maximum of preformation probability for the LCP moves closer to the fission axis and it reaches this axis at tip distance ~ 3 fm between the heavier fragments.

2.3 Review on experimental studies on ternary fission of ^{252}Cf :

Pyatkov *et la*., (2012) reported the results of two different experiments for the study of fission of ^{252}Cf (SF) events in coincidence with neutrons. Two time-of-flight-energy (TOF-*E*) detectors systems have been used. The fission fragment masses were obtained in a double arm coincidence set-up, where the missing mass in the binary decay is used to characterize ternary fission as a collinear cluster tri-partition (CCT). The ^{3}He filled neutron counters have been arranged so as to detect principally neutrons emitted from an isotropic source in the laboratory frame. The fission events

connected to the larger experimental neutron multiplicities show a wide range in the missing-mass spectrum, down to α -particles, carbon and oxygen isotopes. These are linked with magic nuclei in the binary mass-mass correlations of the fission fragments. These neutron-gated data are virtually free from background events from scattered binary fission fragments. The ungated spectra are compared to those of the previous data from our previous article, the observed structures agree well with the manifestations of the collinear cluster tri-partition of ^{252}Cf (SF) observed earlier. Several new families of the CCT modes are observed.

Vermote *et al.*, (2010) determined the emission probabilities and the energy distributions of tritons, α and ^{6}He particles emitted in the spontaneous ternary fission (zero excitation energy) of ^{250}Cf and ^{252}Cf and in the cold neutron induced fission (excitation energy ≈6.5 MeV) of ^{249}Cf and ^{251}Cf. The particle identification was done with suited ΔE–E telescope detectors, at the IRMM (Geel, Belgium) for the spontaneous fission and at the ILL (Grenoble, France) for the neutron induced fission measurements. Hence particle emission characteristics of the fissioning systems ^{250}Cf and ^{252}Cf are obtained at zero and at about 6.5 MeV excitation energies. While the triton emission probability is hardly influenced by the excitation energy, the ^{4}He and ^{6}He emission probability in spontaneous fission is higher than for neutron-induced fission. This can be explained by the strong influence of the cluster preformation probability on the ternary particle emission probability.

Von Oertzen *et al.*, (2010) presented the experimental results in favor of the existence of a new type of cluster decay called “collinear cluster tri-partition”(CCT). They are based on two different experiments with binary coincidences and measurements of the masses and energies of the two fragments, as well as using in one of the experiments observables sensitive to the nuclear charge of the fission fragments. A relatively high yield of the CCT-effect (more than 10^{-3}per binary fission) is likely due to the favourable Q -values (more positive than binary) and is expected due to a collective motion through very elongated (hyper-deformed) pre-scission shapes of the mother system. The process is considered to result from a sequential process, where a heavy cluster (lead as in the case of known cluster radioactivity) is replaced by pairs of two lighter clusters such as the magic isotopes of Sn/Ni or Sn/Ge.

M. Mutterer *et al.*, (2008) measured the energy distribution of the ternary α particles in spontaneous fission of ^{252}Cf. For the first time an energy threshold as low as 1 MeV was reached. In the experimental setup, they have used an array of unshielded silicon detectors measuring energy and time-of-flight (TOF) of ternary particles in coincidence with fission fragments. The TOF resolution of the system was sufficient for clear separation of ^{6}He and tritons from ^{4}He. The statistics were adequate to extract the ^{6}He/^{4}He yield ratio. For both ^{4}He and ^{6}He, excess in the yield (as compared to a Gaussian shape) was observed at energies below 9 MeV. The measured ternary α spectrum was corrected for the distortion induced by the detection geometry covering equatorial particle emission only. The emission angle was found to affect mainly the width of the energy distribution by up to 1 MeV.

Vermote *et al.*, (2008) determined the emission probabilities and the energy distributions of tritons and α particle emitted in the spontaneous ternary fission (zero excitation energy) of ^{244}Cm, ^{246}Cm and ^{248}Cm and in the cold neutron induced fission (excitation energy ≈6.5 MeV) of ^{243}Cm, ^{245}Cm and ^{247}Cm. The particle identification was done with suited $\Delta E-E$ telescope detectors, at the IRMM (Geel, Belgium) for the spontaneous fission and at the ILL (Grenoble, France) for the neutron induced fission measurements. Hence particle emission characteristics of the fissioning systems ^{244}Cm, ^{246}Cm and ^{248}Cm are obtained at zero excitation energy and at excitation energy around 6.5 MeV. Whilst the triton emission probability is hardly influenced by the excitation energy, the ^{4}He emission probability in spontaneous fission is about 20% higher than for neutron-induced fission. This could be explained by the influence of the cluster preformation probability on the ternary α emission.

Ramayya *et al.*, (2006) described the new experiment devoted to the fission of ^{252}Cf. It continued a series of experiments based on correlation measurements of γ rays emitted by fission fragment pairs. The measurements of γ-γ and γ-γ-γ coincidences were done at Gammasphere with closed ^{252}Cf sources. The open source was used for the first time in the last experiment. Fission fragment detectors were arranged in the center hole of Gammasphere. Correlations between fission fragment masses, total kinetic energy, and γ rays were observed. The first, preliminary results of data analysis are discussed.

Oberstedt *et al.*, *(*2005) measured the energy of the light charged particle (LCP) emitted in thermal neutron-induced fission of ^{252}Cf* (E*=6.2 MeV), using the recoil mass-separator **Lohengrin.** For this compound nuclear system emission yields of LCPs, their mean kinetic energies and widths have been obtained for 8 isotopes with nuclear charges $Z \geq 2$. For 13 further isotopes the emission yields were estimated on the basis of systematic on their kinetic energy distributions. ^{34}Al and ^{36}Si emission has been observed for the first time in thermal neutron-induced fission.

Daniel *et al.*, (2004) studied the ternary fission of ^{252}Cf at Gammasphere with eight $\Delta E \times E$ particle telescopes. After Doppler correction, the 3368 keV $2^+ \rightarrow 0^+$ transition in ^{10}Be was found in coincidence with the ^{10}Be fragments with no evidence for any γ rays not Doppler shifted for ^{10}Be with >21 MeV kinetic energy. The ratio of the first 2^+ to ground-state population probabilities was estimated as $N(2^+)/N(0^+)=0.160\pm0.025$. The angular distribution for 3368 keV γ rays indicated the spin alignment of excited ^{10}Be nuclei preferentially is parallel or antiparallel to their momentum.

Hwang *et al.*, (2003) studied He and Be ternary fission processes of ^{252}Cf in two experiments with the Gammasphere detector array with light charged particle detectors surrounding the source. From α-γ double-gated spectra, neutron multiplicity distributions were determined for related α ternary fission pairs. In going from binary to α ternary SF for approximately the same mass splittings (A ≈ 104–146) the average neutron multiplicity decreases about 0.7 amu. In the first light charged particle (LCP) γ-γ experiment, the ^{10}Be spectrum was cutoff below 27 MeV and in the recent experiment, below 18 MeV. For high energy (E > 27 MeV) ^{10}Be ternary fission, the data indicate that the largest yields go via the cold process (zero neutron evaporation). In the recent experiment with E cutoff of 18 MeV, the ^{10}Be ternary SF was observed for zero to 4n emissions. It seems that in some cases like ^{136}Te, the on channel is the strongest and in the other cases like ^{100}Zr the 1n or 2n channel dominates. Clearly, there is a shift to lower average number of neutrons emitted for ^{10}Be compared to α ternary SF. The ^{136}Te is more spherical than the heavy partners in the other pairs and this may influence the 0n channel. Finally, the 0n channel may be more enhanced in the first data with the higher ^{10}Be energy cutoff, leading to lower excitation energy.

Also, they confirmed the 3368 keV peak with the FWHM of 60 keV emitted from the moving Be particles in the Doppler effect corrected spectrum.

Ramayya *et al.*, (2001) studied the spontaneous fission (SF) of ^{252}Cf γ-γ-γ coincidence and light charged particleγ-γ coincidence with Gammasphere. The yields of correlated Mo-Ba pairs in binary fission with 0–10 neutron emission have been remeasured with an uncompressed cube. The previous hot fission mode with 8–10 neutron emission seen in the Mo-Ba split is found to be smaller than earlier results but still present. New 0*n* binary SF yields are reported. By gating on the light charged particles detected in ΔE-E detectors and γ-γ coincidence with Gammasphere, the relative yields of correlated pairs in alpha ternary fission with zero to 6*n* emission are observed for the first time. The peak occurs around the α2*n* channel. A number of correlated pairs are identified in ternary fission with ^{10}Be as the light charged particle. They observed cold, 0*n* ^{10}Be and they also observed hot, *xn* ^{10}Be channels, which may exist in a small amount.

Ramayya *et al.*, (1998) observed experimentally the phenomenon of cold (neutronless) alpha ternary fission in spontaneous fission of ^{252}Cf by triple gamma coincidence technique with Gammasphere with 72 gamma-ray detectors. Correlated pairs of $_{36}$Kr-$_{60}$Nd, $_{38}$Sr-$_{58}$Ce, $_{40}$Zr-$_{56}$Ba, $_{42}$Mo-$_{54}$Xe, $_{44}$Ru-$_{52}$Te, and $_{46}$Pd-$_{50}$Sn were observed to be associated with α ternary fission of ^{252}Cf. Yields of cold α ternary fission were extracted.

Hongyin Han *et al.*, (1997) studied the correlations between the neutron and γ-ray emission and the kinetic energy of light charged particles (LCPs), such as protons, deuterons, tritons and alphas, from the fission of ^{252}Cf in a four-parameter experiment. A circle divide 16 cm × 5 cm liquid scintillator with n-γ discrimination and a circle divide 10 cm × 10 cm NaI(Tl) crystal were employed to detect the neutrons and the γ rays, respectively, while a thin CsI(Tl) crystal, which had the ability to separate the LCPs, was used to determine the LCP energy. The experimental results show that for the α particle accompanied fission, the average total number of neutrons emitted per fission increases in the case of varying the alpha particle energy E_α from 7 to 11 MeV and then falls off linearly in a first approximation with increasing E_α, and the average total energy and the average total number of γ-rays per fission as well as the average

γ-ray energy as functions of E_α show similar correlation features. For the hydrogen-ion accompanied fission, the correlations of the neutron and γ-ray emission with hydrogen ion (t, d and p) energy are very similar to those for the alpha-particle accompanied fission. The correlations of the neutron and γ-ray emission in the low LCP energy region, in contrast to that observed in the high LCP energy range are called anomalies. On the basis of the results obtained by the three-point charge model and the liquid drop model calculation with shell and pairing correction, the anomalous behavior of the neutron and γ-ray emission is explained.

References:

[1]. I.Tsekhanovich, Z. Büyükmumcu, M. Davi, H. O. Denschlag, F. Gönnenwein, and S.F. Boulyga, Phys.Rev.C **67**, 034610 (2003).

[2]. S.L.Whestone and T.D.Thmoas, Phys.Rev.C **154**, 174, 1967. [3]. G.M.Raisbeck and T.D. Thomas, Phys.Rev.C **172**, 1272 (1968).

[4]. V.N.Andreev et al., Sov.J.Nucl.Phys, **8,** 22 (1969).

[5]. A.A.Vorobiev, D.M.Seleversdtov, V.T.Grachov, I.A.Kondurov, Yu.N.Zalite, Phys.Lett B, **40**, 102 (1972).

[6]. G.H.Mehta, J.Poitou, M.Ribrag and C.Signarbieux, Phys.Rev.C **7**, 373 (1973).

[7]. E.Piasecki and J.Blocki, Nucl.phys.A, **208,** 381 (1973).

[8]. Ismail, W.M. Seif, A. Y. Ellithi, A.S. Hashem, Canadian Journal of Physics, 0549 (2013).

[9].K. R. Vijayaraghavan, W. von Oertzen, M. Balasubramaniam, The European Physical Journal A, **48**, 27 (2012).

[10]. V. Mirzaei, H. Miri-Hakimabad, Romanian Reports in Physics **64**, 50 (2012).

[11].K. Manimaran, and M. Balasubramaniam, Physical Review C, **83,** 034609 (2011).

[12]. K Manimaran, M Balasubramaniam, Journal of Physics G: Nuclear and Particle Physics, **37,** 14 (2010).

[13]. K. Manimaran, Balasubramaniam, The European Physics Journal A , **45**, 293 (2010).

[14].K. Manimaran and M. Balasubramaniam,Physical Review C, **79**, 024610 (2009).

[15] J. P. Lestone, Phys. Rev. C **72**, 014604 (2005).

[16].C. Wagemans' J. Heyse, P. Janssens, O. Serot, P. Geltenbort,Nuclear Physics A,**742** 291 (2004).

[17].M. Mutterer, Yu. N. Kopatch, Acta Physica Hungarica A: Heavy Ion Physics **18,** 393, (2003).

[18]. Yu. N. Kopatch, M. Mutterer, D. Schwalm, P. Thirolf, and F. Gönnenwein, Phys. Rev. C **65**, 044614 (2002).

[19].Manfred Mutterer**,** Nuclei Far from Stability and Astrophysics, NATO Science Series **17**, 185 (2001).

[20]. D. S. Delion, A. Florescu, and A. Săndulescu,Phys. Rev. C **63**, 044312 (2001).

[21]. Ş. Mişicu, A. Săndulescu, and W. Greiner, Phys. Rev. C **61**, 041602 (2000).

[22].F. Carstoiu, I. Bulboacă, A. Săndulescu, and W. Greiner, Phys. Rev. C **61**, 044606 (2000).

[23].J. K. Hwang, A. V. Ramayya, J. H. Hamilton, C. J. Beyer, J. Kormicki, Phys. Rev. C **61**, 047601 (2000).

[24]. A. Săndulescu, F. Carstoiu, I. Bulboacă, and W. Greiner, J.Phys. Rev. C **60**, 044613 (1999).

[25].D. N. Poenaru, W. Greiner, J. H. Hamilton, A. V. Ramayya, E. Hourany, and R. A. Gherghescu, Phys. Rev. C **59**, 3457 (1999).

[26].A.Florescu, A. Sandulescu, A. J. Delion, D.S. Hamilton, J.H. Ramayya, A.V. Greiner, W. ©2011 American Physical Society, **31,** 31010980 (1999).

[27].Yu.V. Pyatkov, D. V. Kamanin, W. von Oertzen, A. A. Alexandrov, I. A. Alexandrova, The European Physical Journal A, **48,** 94 (2012).

[28].S. Vermote ,C. Wagemans, O. Serot, J. Heyse, J. Van Gils, et al., Journal of Nuclear**, 837**,176 (2010).

[28]. W. von Oertzen, A. A. Alexandrov, I. A. Alexandrova, O. V. Falomkina, N. A. Kondratjev, The European Physical Journal A **45**, 29 (2010).

[29]. M. Mutterer, Yu. N. Kopatch, S. R. Yamaledtinov, V. G. Lyapin, J. von Kalben, et al., Phys. Rev. C **78**, 064616 (2008).

[30]. S. Vermote, C. Wagemans, O. Serot, J. Heyse , J. Van Gils, Nuclear Physics A **806**,1-14 (2008).

[31]. C. Goodin, D. Fong, J. K. Hwang, A. V. Ramayya, J. H. Hamilton, et al., Phys. Rev. C **74**, 017309 (2006).

[32]. S. Oberstedt, S. Raman, D. Rochman, F. Gönnenwein, I. Tsekhanovich, et al., Nuclear Physics A, **761**,173 (2005).

[33]. A. V. Daniel, G. M. Ter-Akopian, J. H. Hamilton, A. V. Ramayya, J. Kormicki, et al.,Phys. Rev. C 69, 041305 (2004).

[34]. J. K. Hwang, D. Fong, A. V. Ramayya, J. H. Hamilton, M. Jandel, Acta Physica Hungarica A: Heavy Ion Physics, **18**, 393 (2003).

[35].A.V. Ramayya, J.H. Hamilton, J.K. Hwang, C.J. Beyer, G.M. Ter Akopian, Progress in Particle and Nuclear Physics,**46**,221 (2001).

[36].Hamilton.J.H, Ramayya. A. V, Hwang .J. K, Kormicki .J, Babu. B. R. S,Phys. Rev. C **57**, 2370 (1998).

[37].Hongyin Han, Shengnian Huang, Guanren Shen, Ying Qiao, Gang Sun,Nuclear Physics A **615**, 162 (1997).

CHAPTER-III
METHODOLOGY

3.1 Introduction:

Fission is a binary process, in which two nuclei of comparable mass (the primary fission fragments) are formed after the splitting of the parent nucleus. Much less frequently, more than two nuclei are formed and if precisely three nuclei appear, the fission event is classified as a ternary event. Ternary fission is defined as the breakup of heavy nuclei into three fragments of approximately equal mass. Here, uncharged particles such as multiple neutrons and gamma-rays are produced in ternary fission. A ternary fission process occurs once every few hundred of fission events. About 25% more ternary fission present in spontaneous fission compared to the same fissioning system formed after thermal neutron capture. The most important light-charge-particle accompanied in the process of ternary fission is alpha-particle; indeed about 90% of the ternary particles are alpha- particles and about 10% tritons, the remaining fraction being constituted by a large variety of particles. In this sense, small traces of emission of light-charge-particles like isotopes of H, He, Be were observed in the spontaneous ternary fission of ^{252}Cf [1].

The energy spectrum of the alpha- particle stemming out in ternary fission is very long and is ranging from 6 to 38 MeV. Such energetic alpha particles have long range, which differs from the less energetic short-range alpha particles, emitted from the radioactive alpha-decay. As evidenced by the experimental angular distribution, the light ternary particles are emitted about perpendicular to the fission axis. This represents an indication that the light particle is formed in the median region between the heavy fragments. A very rare type of ternary fission process is sometimes called “true ternary fission”. It produces three nearly equal sized charged fragments (Z-30) but only happens in about one in 100 million fission events. In true ternary fission, the product nuclei split the fission energy in three nearly equal parts and have kinetic energies of ~60 MeV. In this chapter the binding energy, coulomb potential, proximity potential and fragmentation potential and three cluster model are explained.

3.2 Binding Energy (BE)

The mass defect of a nucleus is the differences between the mass of a nucleus and the mass of its constituent protons and neutrons [2]. The energy equivalent of this mass difference ($\Delta E=\Delta mc^2$) is known as the binding energy of the nucleus. The binding energy of a nucleus is defined as the work done to separate a nucleus into its constituent neutrons and protons. The magnitude of the binding energy of a nucleus determines its stability against disintegration. If binding energy greater than zero, the nucleus is stable and energy must be supplied from outside to disrupt it into its constituents. If binding energy less than zero, the nucleus is unstable and it will disintegrate by itself [3].

The formula represented by the binding energy (BE) is

$$BE = (\Delta M)\, C^2 \text{ MeV}.$$

$$BE = (Zm_P+Nm_n-M) \text{ x } 931.494 \text{ MeV} \text{ ---------- } (3.1)$$

Where, Z is the number of the proton.

m_p is the mass of the proton.

N is the number of the neutron.

m_n is the mass of the neutron.

M is nuclear mass.

ΔM is the mass defect.

C is the velocity of light ($3x10^8$m/sec)

Masses are in atomic mass unit.

The obtained binding energy value is checked with experimental values [9],[10] and mean values are taken from[9],[10].

3.3 Mass Asymmetry

If the parent nucleus A disintegrates into the possible combination A_1, A_2, then the quantity mass asymmetry is defined,

$$\eta = \frac{A_1 - A_2}{A_1 + A_2}$$

These combinations of masses are charge minimized [11].

3.4 Coulomb Potential (V_c):

The expression for maximum potential energy at $R_{ij} = R$ which is the sharp contact point of the emitted fragments,

$$V_{c(ij)} = Z_i Z_j e^2/R_{ij} \text{ (MeV)} \quad (ij = 12,23,13) \text{---------- (3.2)}$$

$R_{ij} = R_i + R_j$ (fm). Where R_{ij} is the distance between the centers of the interaction fragments. R_i is the radius of i^{th} nuclei (i = 1, 2, 3) and is given by

$$R_i = 1.28A_i^{1/3} - 0.76 + 0.8A_i^{1/3} \text{ fm}$$

and similarly R_i is radius of the j^{th} nuclei (j = 1,2,3) (fm).

where, Z_1, Z_2, are the charge numbers of the respective fragments.

$$e^2 = 1.44 \text{MeV fm.}$$

and Fig .3.1 shows ternary configuration.

For binary system, Coulomb potential is $Vc_{(12)} = Z_1 Z_2 e^2/R_{ij(12)}$

$$Vc_{(23)} = Z_2 Z_3 e^2/R_{ij(23)}$$

$$Vc_{(31)} = Z_3 Z_1 e^2/R_{ij(31)}$$

The coulomb potential is calculated for ternary fission in collinear configuration as shown in figure 3.1.

For ternary fission, the coulomb potential $V_c = Vc_{12} + Vc_{23} + Vc_{13}$ ---------- (3.3)

3.5 Proximity potential (V_p)

The concept of the proximity potential has come to play an important role in the Physics of heavy ion collisions. Blocki et al. first introduced it, in the calculation of heavy ion potentials. It has now been extended to the collision of deformed, oriented nuclei. The proximity potential is a surface effect; in judging the effectiveness of such an approach (and of the interaction itself) it should be useful to examine not only the microscopic nucleus-nucleus interaction potential but also how well the method is able to reproduce the surface energy coefficient in the binding energy expression for the nuclei [8]. All proximity potential is based on the proximity force theorem. According to which "The force between two gently curved surfaces in close proximity is proportional to the interaction potential per unit area between the two flat surfaces". The nuclear part of the representing the mean curvature of the interaction surfaces and universal function depending on the separation distance [5].

When two surface approach each other within a small distance of ~ 2 to 3 fm, comparable with the surface thickness of interacting nuclei, or when a nucleus is at

the verge of dividing into two surface actually face each other across a small gap or crevice. In both the cases, the surface energy term alone could not give rise to the strong attraction that is observed when the two surfaces are brought in close proximity. Such additional attractive forces are called proximity forces and the addition potential due to these forces is called the proximity potential [6].

The proximity potential V_p for spherical fragments, according to Blocki et al.,[7] is

$$V_p = 4 \Pi \bar{R} \gamma b \Phi(\xi) \quad \text{---------- (3.4)}$$

$\Phi(\xi)$ is the universal function of proximity potential, which depends only on the distance between two nuclei and is independent of the charge numbers of the two nuclei, given as

For $\xi \leq 1.251$,

$$\Phi(\xi) = -1/2(\xi-2.54^2 -0.0852(\xi-2.54)^3.$$

For $\xi \geq 1.251$,

$$\Phi(\xi) = -3.437\exp(-\xi/0.75).$$

Here, ξ = s/b. This function is defined for negative (the overlap region), zero (touching configuration) and positive (separated configuration) values of s. The value of the diffuseness of the nuclear surface is b~1 fm. The factor γ is the specific nuclear surface co-efficient given by

$$\gamma = 0.9517[1-1.7826(N-Z/A)^2] \text{ MeV fm}^{-2}$$

$N = N_1+N_2$ and $Z = Z_1+Z_2$ represent neutron number and proton number of the parent nucleus respectively. A is the mass number of the parent nucleus.

In equation $\bar{R}$ is the mean curvature radius of the reaction partners, characterizing the gap which for spherical nuclei is given by $\bar{R} = C_iC_j/C_i+C_j$ fm. Assuming that the third particle is formed collinearly in between the main two fragments, the neck radius becomes equal to the radius of the third fragment. As shown in Figure 3.1, radius of the first second and third fragments are denoted by R_1,R_2,R_3.

R_{12},R_{23},R_{13} are the distances between the fragments 1and 2, 2 and 3, 1 and 3 respectively.

$$R_{12} = R_1 +R_2$$

$$R_{23} = R_2+R_3$$

$$R_{13} = R_1 +R_3$$

The unit of R is fermi (fm). C_i(i=1,2,3) are the Sussman's central radii and related to the effective sharp radii $R_i = 1.28A_i^{1/3}-0.76+0.8A_i^{-1/3}$ fm

$$C_i = R_i (1-b^2/R_i^2) \text{ fm.}$$

$$C_j = R_j (1-b^2/R_j^2) \text{ fm.}$$

$$C_{ij} = C_i + C_j$$

For binary system, proximity potential $V_{p\,(12)} = 4\,\Pi\,\bar{R}_{(12)}\,\gamma_{12}\,b\Phi(\xi)$

$$V_{p\,(23)} = 4\,\Pi\,\bar{R}_{(23)}\,\gamma_{23}\,b\Phi\,(\xi)$$

$$V_{p\,(23)} = 4\,\Pi\,\bar{R}_{(31)}\,\gamma_{23}\,b\Phi\,(\xi)$$

For ternary Fission, proximity potential $V_p = V_{p\,(12)} + V_{p\,(23)} + V_{p\,(23)}$ ---------- (3.5)

So that, Fragmentation potential for ternary fission is sum of binding energy (BE),coulomb potential (V_c), and proximity potential ($V_{p)}$ and it is denoted by $V_{(\eta\eta)}$.

Fragmentation potential is $V_{(\eta\eta)} = BE + V_c + V_p$ ---------- (3.6)

3.6 Model

In the Unified Fission Model (UFM), the cluster decay is dealt simply as a barrier penetration problem where as the preformed cluster model (PCM) distinguishes itself from the unified fission model (UFM) in its basic assumption of the emitted cluster(s) being preborn in the parent nucleus with a probability that decreases with the increasing size of the cluster [23]. This suggests that the process of cluster decay will stop somewhere and that of fission will take over, with a possible overlap for some region. It is seen that such an overlap does exist indeed for clusters of masses $42 < A_2 < 50$. The UFM is a fission model in which the cluster formation probability is calculated as the cluster barrier penetration, whereas in PCM the cluster preformation is calculated by solving the Schrödinger equation for the dynamic flow of charges and masses. In both the

models, UFM and PCM the cluster is supposed to penetrate the potential barrier with available Q value, which also play a vital role in calculating the half lives of the emitted cluster .The preformation probability varies from cluster to cluster. The PCM is developed as a further modification of the Gamow theory, considering not only the penetration of a realistic barrier (coulomb + nuclear, as in UFM), but also associating a preformation probability $P_0$to the emitting cluster. Thus, the decay constant in the PCM is defined by $\lambda_{PCM} = \upsilon_0 P P_0$.

3.7 Three cluster model (TCM)

The three-cluster model developed as an extension of the preformed cluster model (PCM) of Gupta and collaborators for ground-state decays in cluster radioactivity (CR) and related phenomena [12–16]. Thus, like PCM, TCM is also based on the dynamical or quantum mechanical fragmentation theory of cold fusion phenomenon in heavy-ion reactions and fission dynamics, including the prediction of CR [16-22]. The three-cluster model is used to explain the ternary fission of heavy radioactive nuclei based on the cluster picture. Within this model for a fixed third fragment, one can calculate the fragmentation potential minimized in mass and charge asymmetry coordinates and one can study systematically the probability of fragments and isotopic yield of ternary fission of given nucleus.

In the present work, the fragmentation potential is calculated based on three cluster model for the ternary decay of ^{252}Cf, by fixing the third particle using the equation (3.6). The calculations were carried out using the FORTRAN programming language.

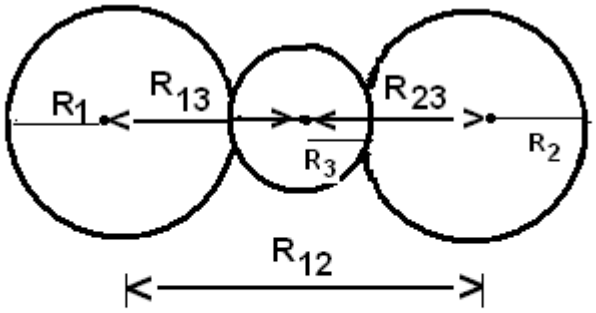

Figure 3.1 Schematic touching configuration in the case of collinear emission.

References:

[1]. V.Mirzaei, H.Miri-Hakimabad, Romanian Reports in Physics, **64,** 50 (2012).

[2]. Jim Breithaupt, Physics, Palgrave publishers Ltd, 344 (2002).

[3]. A.K. Saxena, Principles of modern physics second edition, Narosa publishing house, 13.9 (2007).

[4].Tom Duncan, Advanced physics fourth edition, John Murray publishing Ltd, 515 (1994).

[5]. Ishwar Dutt and Rajeev K. Puri, Phys.Rev C **81**, 064608 (2010).

[6]. Ishwar Dutt and Rajeev K. Puri, Phys.Rev C **81**, 064609 (2010).

[7]. J.Blocki, J.Randrup, W.J.Swiatecki, and C.F.Tsang, Ann. Phys. (NY) **105,** 427(1977).

[8]. A.J.Baltz and B.F Bayman, Phys. Rev C **26**, 1969 (1982).

[9]. A. Audi and A.H.wapstra, Nucl.phys.A, **729**, 676 (1995).

[10]. P.Moller, J.R.Nix, W.D.Myers and W.J.Swiateck, At. Data nucl.data tables, **59**, 185 (1995).

[11]. N.S. Rajeswari, K.R.Vijayaraghavan and M. Balasubramaniam, Eur. Phys. J. A. **47,** 126 (2011).

[12]. R. K. Gupta, in Proceedings of the 5th International Conference on Nuclear Reaction Mechanisms, 416 (1988).

[13]. S.S. Malik and R. K. Gupta, Phys. Rev. C **39**, 1992 (1989).

[14]. R. K. Gupta, W. Scheid, and W. Greiner, J. Phys. G: Nucl. Part.Phys.**17**,1731(1991) [15]. S. Kumar and R. K. Gupta, Phys. Rev. C **49**, 1922 (1994).

[16]. R. K. Gupta, In Heavy Elements and Related New Phenomena, **2**, 730 (1999).

[17]. R.K.Gupta, Sov. J. Part. Nucl.**8**, 289 (1977).

[18].J. A. Maruhn, W. Greiner, and W. Scheid, in Heavy Ion Collisions, 2, Chapter 6 (1980).

[19]. A.Sandulescu, D. N. Poenaru, and W. Greiner, Sov. J. Part.Nucl.**11**, 528 (1980).

[21]. R. K. Gupta and W. Greiner, in Heavy Elements and Related New Phenomena, **1,** 536 (1999).

[22].H. Kröger and W. Scheid, J. Phys. G **6,** L85 (1980).

[23]. K. Manimaran and M. Balasubramaniam, Phys Rev.C **79**, 024610 (2009).

CHAPTER IV
RESULTS AND DISCUSSION

4.1 He accompanied Ternary Fission

The fragmentation potential is calculated for the ternary decay of the parent nuclei ^{252}Cf. Calculations were carried out by fixing third particle. By fixing third particle and other two particles are charge minimized. The fragmentation potential is calculated using equation (3.6), which is described in the Chapter-III. The fixed third particle are isotopes of He (^{3}He,^{4}He,^{5}He,^{6}He,^{7}He,^{8}He), isotopes of Be (^{7}Be,^{8}Be,^{9}Be,^{10}Be,^{11}Be,^{12}Be,^{13}Be) C(^{9}C,^{10}C,^{11}C,^{12}C,^{13}C,^{14}C,^{15}C) and Mg(^{21}Mg,^{22}Mg,^{23}Mg,^{24}Mg,^{25}Mg,^{26}Mg,^{27}Mg). In figure 4.1 ^{3}He is fixed as third particle that shows the preference for^{245}Pu+^{4}He in the lighter mass region, ^{167}Gd+^{82}Ge is preferred in the asymmetric mass region and ^{132}Sn+^{111}Pd in the symmetric mass region. In figure 4.2 ^{3}He replaced by ^{4}He as a third particle, in which ^{244}Pu+^{4}He is preferred in the lighter mass region, than ^{166}Gd+^{82}Ge in the asymmetric mass region as well as in the symmetric mass region ^{132}Sn+^{116}Pd is preferred. Our result^{132}Sn+^{116}Pd are confirmed with author [1]. In next figure 4.3 third particle is chosen as ^{5}He so that, lowest fragmentation potential value occurs for ^{243}Pu+^{4}He in the lighter mass region, ^{165}Gd+^{82}Ge on asymmetric mass region and ^{131}Sn+ ^{116}Pd in symmetric mass region.

In figure 4.4 ^{6}He is fixed as a third particle ^{242}Pu+^{4}He is preferred in the lighter mass region, the probability is more for ^{164}Gd+^{82}Ge in the asymmetric mass region and ^{130}Sn+^{116}Pd in the symmetric mass region. When ^{7}He is chosen as third particle, there is occurs of ^{241}Pu+^{4}He in lighter mass region,^{163}Gd+^{82}Ge on asymmetric mass region and in the symmetric region ^{131}Sn+^{114}Pd is preferred. In figure 4.6 ^{8}He placed as the third particle so that, there is more probability for ^{240}Pu+^{4}He in the lighter mass region,^{162}Gd+^{82}Ge in the asymmetric mass region and ^{134}Te+^{110}Ru in the symmetric mass region. Here different result is obtained from the result He isotopes in the symmetric mass region the preferred nuclei are Sn and Pd, whereas for ^{8}He as third particle ^{134}Te+^{110}Ru is preferred. Further it is noted from the figure4.7 which shows the fragmentation potential of all the isotopes of He (^{3}He,^{4}He,^{5}He,^{6}He,^{7}He,^{8}He). The ^{3}He fixing as third particle fragmentation potential

has lowest value. But expected, ^{4}He is the most preferred configuration. it needs further investigation[1].

4.2 Be accompanied Ternary Fission

In second step, Be isotopes (^{7}Be,^{8}Be,^{9}Be,^{10}Be,^{11}Be,^{12}Be,^{13}Be) are fixed as third particle and the remaining combination of A_1, A_2 are charge minimized. Consider ^{7}Be as a fixed third particle is shown in figure 4.8 here ^{241}U+^{4}He, ^{163}Sm+^{82}Ge, ^{132}Sn+^{113}Ru are preferred in the lighter mass region, asymmetric mass region, symmetric mass region respectively. In figure 4.9 is drawn by considering ^{8}Be as the third particle in which ^{240}U+^{4}He, ^{162}Sm+^{82}Ge, ^{132}Sn+^{112}Ru, are preferred in the above mentioned three main regions. In figure 4.10 is obtained by fixing ^{9}Be as the third particle. Figure 4.10 shows that ,^{239}U+^{4}He, ^{161}Sm+^{82}Ge, ^{132}Sn+^{111}Ru are preferred in lower mass region, asymmetric mass region, symmetric mass region.^{238}U+^{4}He, ^{160}Sm+^{82}Ge, ^{131}Sn+^{111}Ru have lower potential in the above mentioned three main region respectively which is as shown in figure 4.11. Figure 4.11 is drawn by fixing ^{10}Be as the third particle. Our result^{131}Sn+^{111}Ru are conformed to authors [4]. Figure 4.12 is drawn for the ^{11}Be accompanied ternary fission of ^{252}Cf from which the combinations ^{237}U+^{4}He, ^{150}Sm+^{82}Ge, ^{131}Sn+^{110}Ru have the lower potential in lower mass region, asymmetric mass region, and symmetric mass region respectively. Figure 4.13 is drawn by fixing ^{12}Be as the third particle which reveals that ^{236}U+^{4}He, ^{158}Sm+^{82}Ge is ^{134}Te+^{106}Mo are the favored combinations in the above mentioned three mass region respectively. From the figure 4.14 ^{235}U+^{4}He, ^{152}Nd+^{87}Se, ^{134}Te+^{105}Mo are preferred over other combinations in lower mass region, asymmetric mass region, and symmetric mass region respectively for ^{13}Be as the third particle.

Till ^{11}Be for ^{7}Be to ^{11}Be, the combination of A_1+A_2 preferred in the symmetric mass region was Sn+Ru whereas, for the third particle ^{12}Be and ^{13}Be, the combination in symmetric mass region are Te+Mo and in ^{13}Be the asymmetric mass region have the element is different compared to remaining of above mentioned Be isotopes. Here ^{152}Nd+^{87}Se is preferred, above are isotopes Sm+Ge. Figure 4.15 shows that the fragmentation potential of all the isotopes of Be such as (^{7}Be,^{8}Be,^{9}Be,^{10}Be,^{11}Be,^{12}Be,^{13}Be) Fragmentation potential for the third particle ^{10}Be

is found, to have the lowest value. Our results confirm the preference for ^{10}Be accompanied ternary fission of ^{252}Cf with the works of [2], [3].

4.3 Carbon accompanied Ternary Fission

Carbon (^{14}C) is the first cluster to be observed in the cluster radioactivity. So, isotopes of C are considered as third particle. ^{9}C is fixed as the third particle as shown in figure 4.16. Here, ^{240}Pa+^{3}H is preferred in the lighter mass region, then in the asymmetric mass region ^{163}Sm+^{80}Zn and in symmetric mass region ^{132}Sn+^{111}Mo is preferred combination. When the third particle ^{10}C, the result of the fragmentation potential is shown in figure 4.17. The figure 4.17, ^{238}Th+^{4}He in the lighter mass region, in the asymmetric mass region there is preference of ^{162}Sm+^{80}Zn and in the symmetric mass region ^{132}Sn+^{110}Mo is preferred. ^{11}C is present as three particle as shown in figure 4.18,^{237}Th+^{4}He is preferred in lighter mass region, ^{161}Sm+^{80}Zn in the asymmetric mass region and ^{132}Sn+^{109}Mo is found in the symmetric mass region. In figure 4.19, ^{12}C is fixed as third particle, in the lighter mass region ^{236}Th+^{4}He is occurred, there is preference of ^{158}Nd+^{82}Ge on asymmetric mass region and ^{132}Sn+^{108}Mo in the symmetric mass region. In ^{12}C the symmetric mass region is verified with the work of [4]. when ^{13}C is chosen as an third particle is shown in figure 4.20, ^{236}Pa+^{3}H preferred in the lighter mass region, then in the asymmetric mass region ^{157}Nd+^{82}Ge and ^{132}Sn+^{107}Mo in the symmetric mass region are the most probable combination. In figure 4.21 ^{14}C is fixed as third particle ^{234}Th+^{4}He is preferred in the lighter mass region, ^{156}Nd+^{82}Ge lies in the asymmetric mass region and ^{132}Sn+^{106}Mo in symmetric mass region. In figure 4.22, ^{15}C is placed, as the third particle. The probability is more for ^{233}Th+^{4}He occurs in the lighter mass region, ^{155}Nd+^{83}Ge in the asymmetric mass region and ^{132}Sn+^{105}Mo preferred in the symmetric mass region. For the combination ^{9}C and ^{13}C, in the lower mass region, the preferred is for ^{3}H as a second fragment, instead of expected ^{4}He. This may be the element has odd mass number 9 and 11 of the third particle. Further it is noted from figure 4.23 which shows the fragmentation potential of all the isotopes of C (^{9}C,^{10}C,^{11}C,^{12}C,^{13}C,^{14}C,^{15}C).fragmentation potential for the third particle ^{14}C has lowest potential. Our results confirm the preference for ^{14}C accompanied ternary fission of ^{252}Cf with work of [5].

4.4 Mg isotopes accompanied Ternary Fission Fragmentation potential for Mg isotopes are explained given below. Here fixed third particle are Mg isotopes. In figure4.24 by fixing ^{21}Mg as the third particle in which ^{227}Po+^{4}He, ^{151}Ba+^{80}Zn and ^{132}Sn+^{99}Kr are preferred in the lighter mass region, asymmetric mass region and symmetric mass region respectively. In figure 4.25 is drawn by consider ^{22}Mg as the third particle in which ^{224}Po+^{6}He, ^{150}Ba+^{80}Zn and ^{132}Sn+^{98}Kr are preferred in the above mentioned three mass regions. Figure 4.26 is obtained by fixing ^{23}Mg as the third particle that shows ^{225}Po+^{4}He, ^{149}Ba+^{80}Zn and ^{132}Sn+^{97}Kr are preferred in the lighter mass region, asymmetric mass region and symmetric mass region respectively. ^{224}Po+^{4}He, ^{148}Ba+^{80}Zn and ^{132}Sn+^{96}Kr have lower potential in the above mentioned three mass regions respectively which is shown in figure 4.27. Here fixing third particle is ^{24}Mg. Figure 4.28 is drawn for the ^{25}Mg accompanied ternary fission of ^{252}Cf from which the combinations^{223}Po+^{4}He, ^{147}Ba+^{80}Zn and ^{132}Sn+^{95}Kr have the lower potential in the lighter mass region, asymmetric mass region and symmetric mass region respectively. Figure 4.29 is drawn by fixing ^{26} Mg as the third particle, which reveals that ^{222}Po+^{4}He, ^{152}Ce+^{74}Ni and ^{133}Sn+^{93}Kr are the favored combinations in the above mentioned three mass regions respectively. From the figure 4.30, ^{221}Po+^{4}He, ^{153}Ce+^{72}Ni and ^{133}Sn+^{92}Kr are preferred over other combinations in lower mass region, asymmetric mass region and symmetric mass region respectively for fixing ^{27}Mg as the third particle. In figure 4.29, 4.30 shows the Ce+Ni in the preferred combination in asymmetric mass region for the ^{26,27}Mg accompanied ternary fission of ^{252}Cf whereas, Ba+Zn in the preferred combination in asymmetric mass region for the other isotopes of Mg. Fragmentation potential with respect to A_2 for fixing the isotopes of Mg as third particle shows in the figure 4.31. The fragmentation potential for the third particle ^{27}Mg is found that nuclei have the lower potential compared to other isotopes of Mg.

4.5 ^{3}He, ^{10}Be, ^{14}C, ^{27}Mg accompanied Ternary Fission

From figure 4.1 to 4.31, the most probable combination with respect to each isotope like ^{3}He, ^{10}Be, ^{14}C, ^{27}Mg as third particle plotted in a single graph as shown in figure 4.32. Here ^{10}Be as third particle has got the lowest fragmentation potential so, it is concluded that for the decay of ^{252}Cf into three particle breakup, ^{10}Be is preferred as the third particle, which confirms the results by [6].

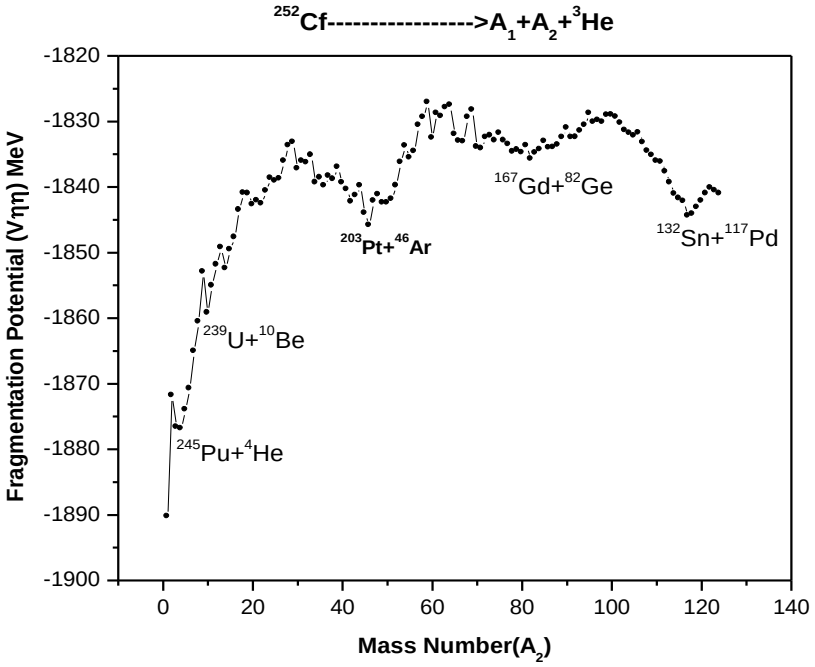

Figure 4.1 Fragmentation potential plotted with respect to A_2 for ^{3}He fixed as a third particle.

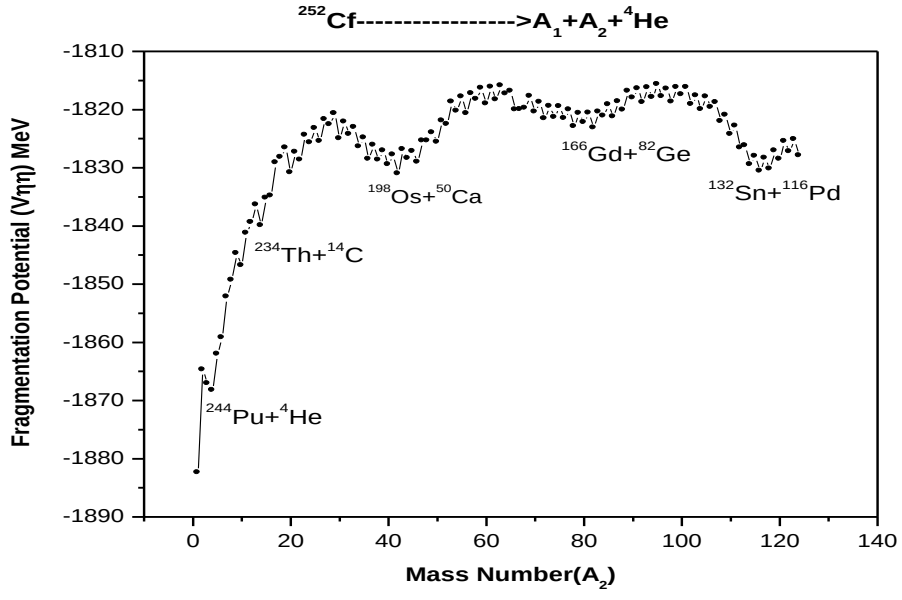

Figure 4.2 Fragmentation potential plotted with respect to A_2 for ^{4}He fixed as a third particle.

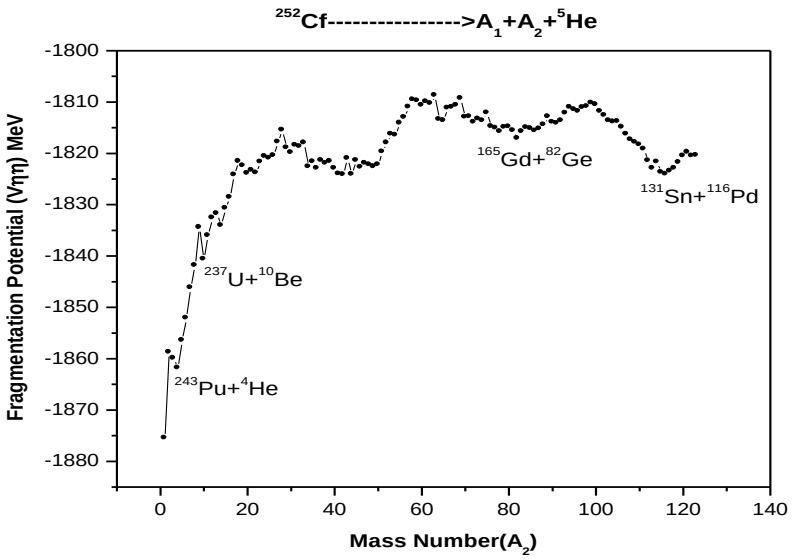

Figure 4.3 Fragmentation potential plotted with respect to A_2 for ^{5}He fixed as a third particle.

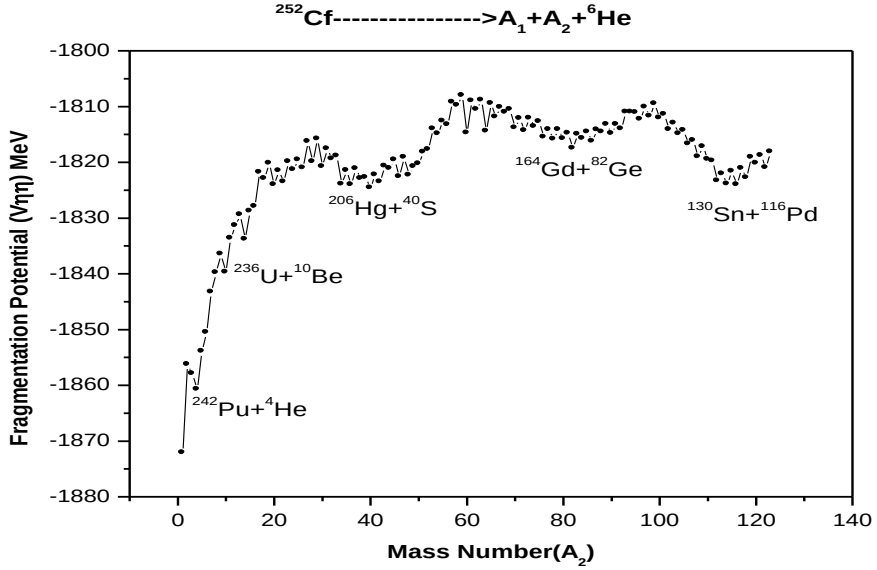

Figure 4.4 Fragmentation potential plotted with respect to A_2 for ^{6}He fixed as a third particle.

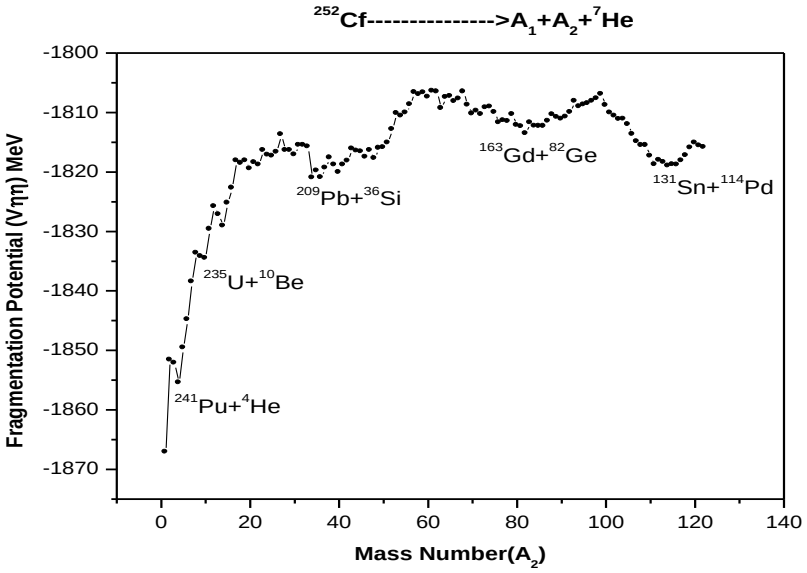

Figure 4.5 Fragmentation potential plotted with respect to A_2 for ^{7}He fixed as a third particle.

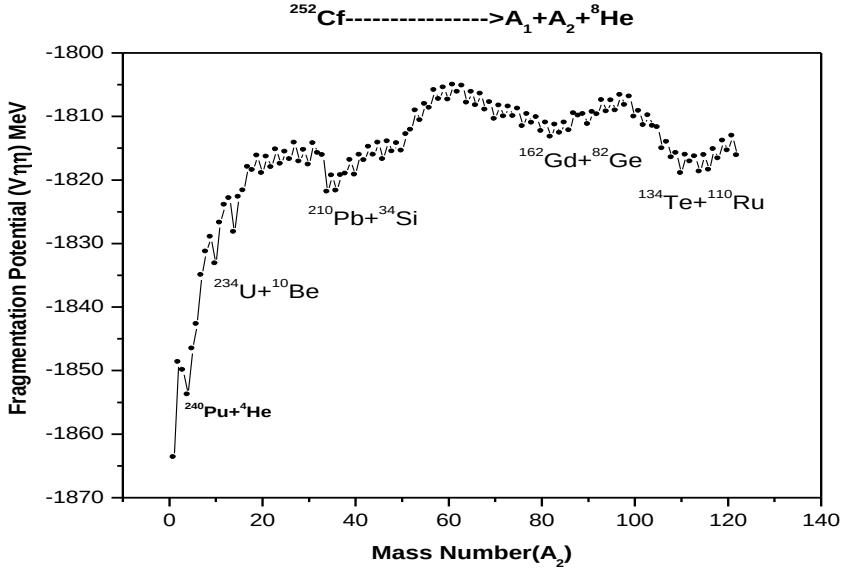

Figure 4.6 Fragmentation potential plotted with respect to A_2 for ^{8}He fixed as a third particle.

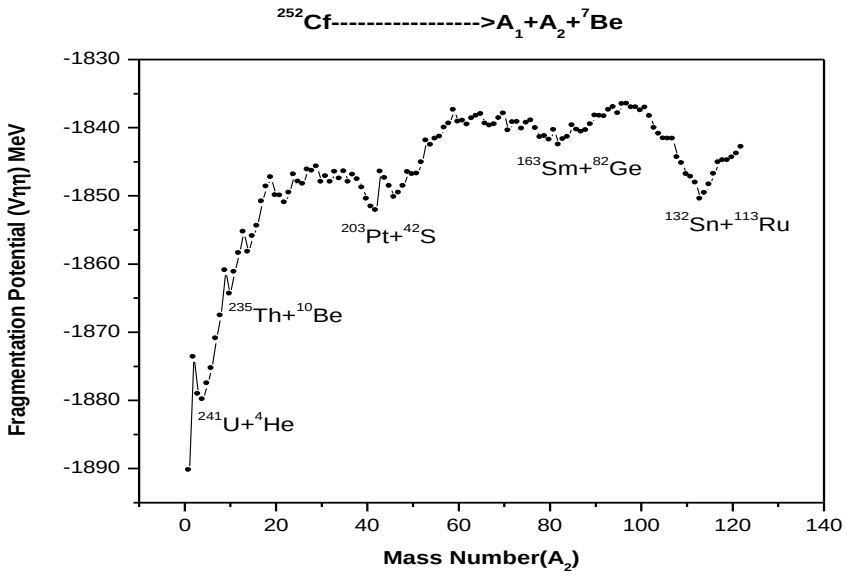

Figure 4.6 Fragmentation potential plotted with respect to A_2 for ^{7}Be fixed as a third particle

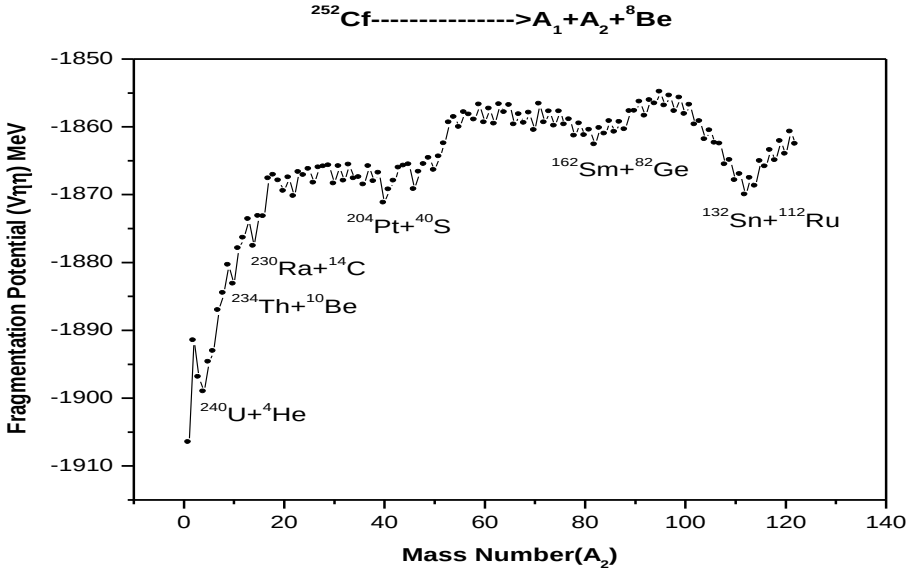

Figure 4.6 Fragmentation potential plotted with respect to A_2 for ^{8}He fixed as a third particle.

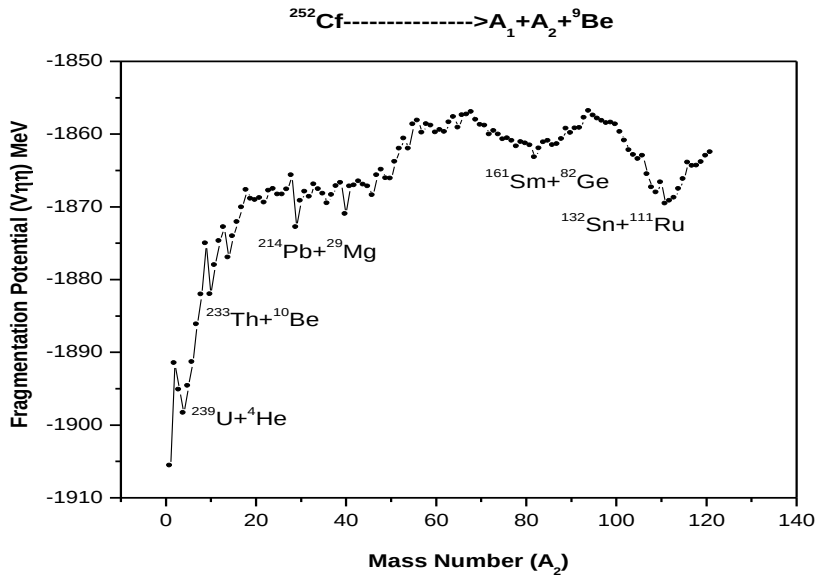

Figure 4.6 Fragmentation potential plotted with respect to A_2 for ^{9}Be fixed as a third particle.

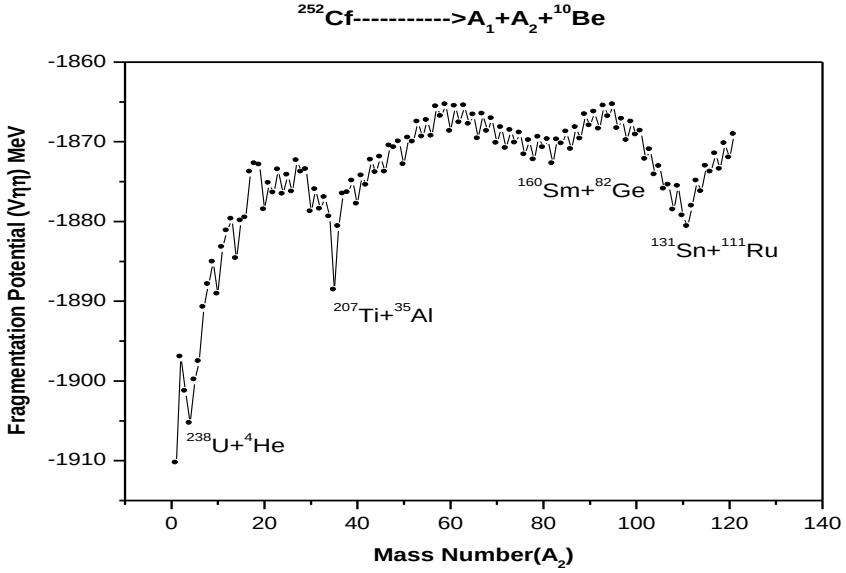

Figure 4.6 Fragmentation potential plotted with respect to A_2 for ^{10}Be fixed as a third particle.

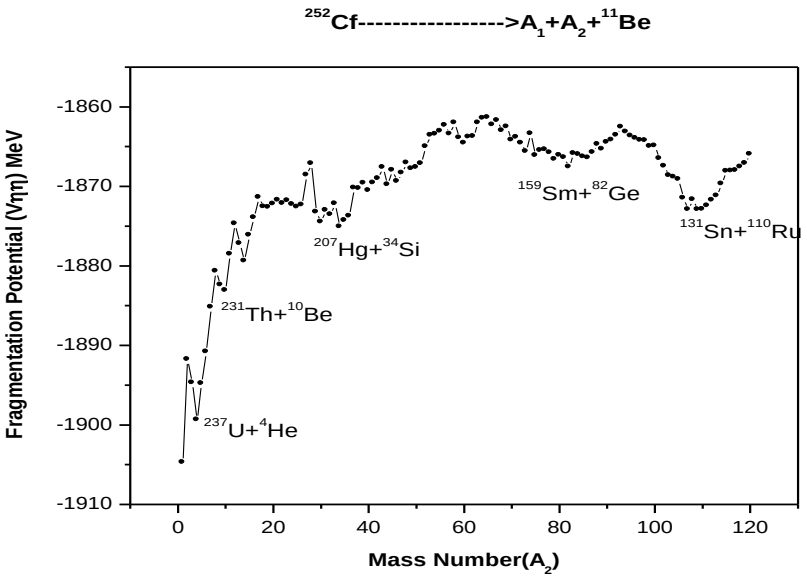

Figure 4.6 Fragmentation potential plotted with respect to A_2 for ^{11}Be fixed as a third particle

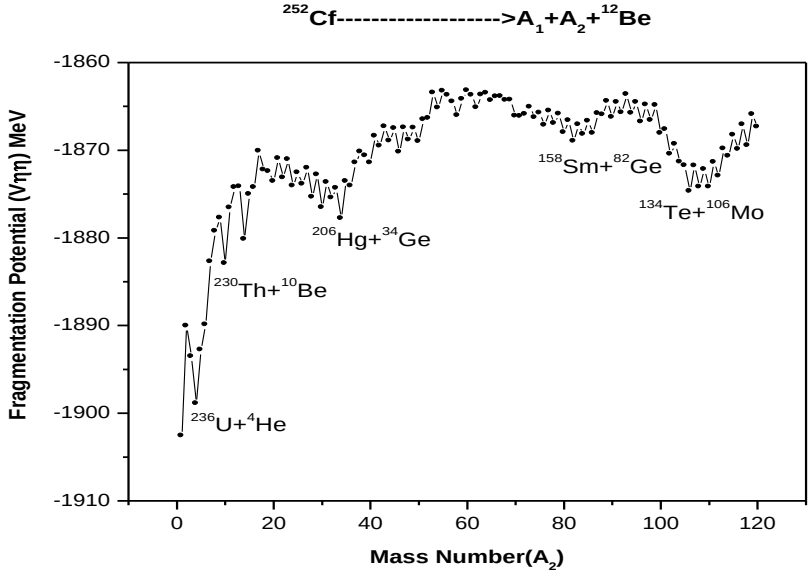

Figure 4.6 Fragmentation potential plotted with respect to A_2 for ^{12}Be fixed as a third particle.

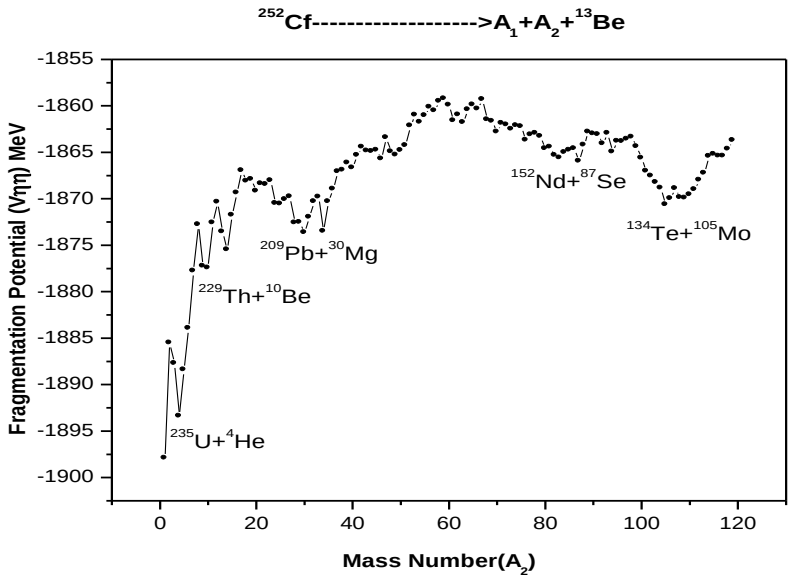

Figure 4.6 Fragmentation potential plotted with respect to A_2 for ^{13}Be fixed as a third particle.

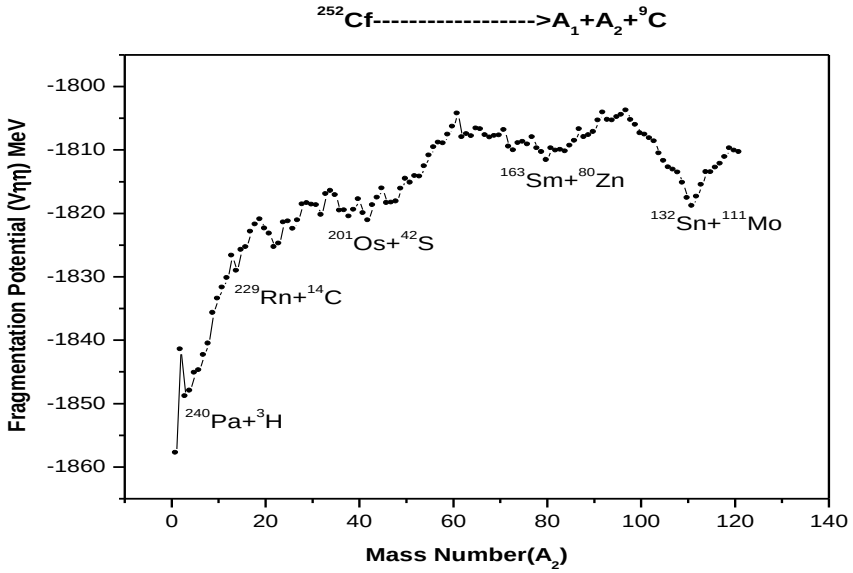

Figure 4.6 Fragmentation potential plotted with respect to A_2 for ^{9}C fixed as a third particle.

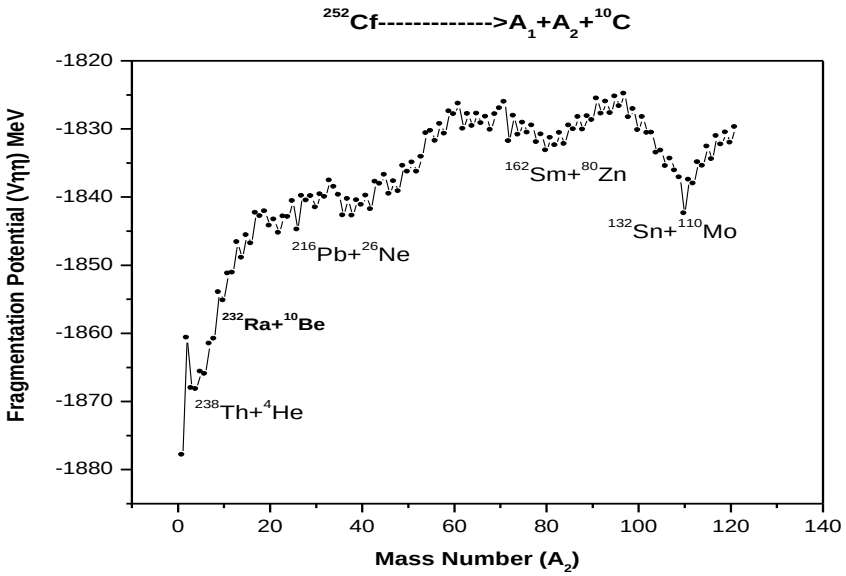

Figure 4.6 Fragmentation potential plotted with respect to A_2 for ^{10}C fixed as a third particle.

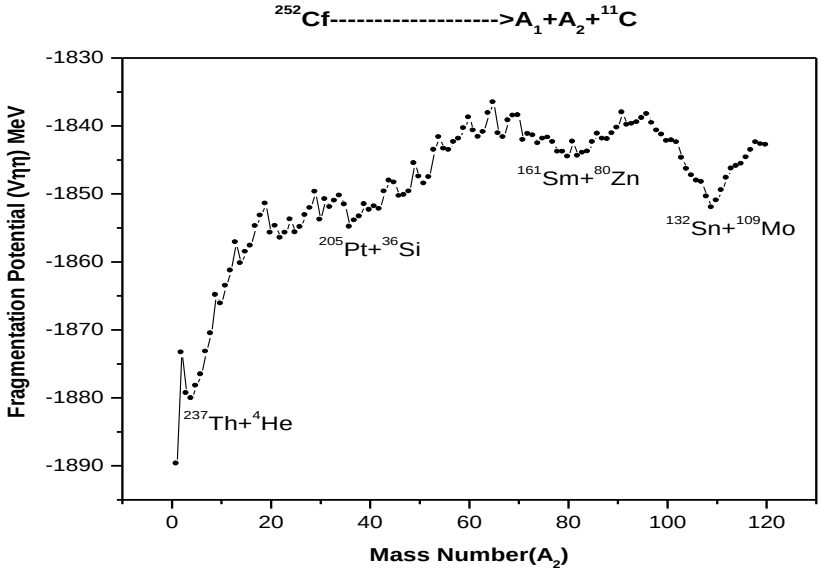

Figure 4.6 Fragmentation potential plotted with respect to A_2 for ^{11}C fixed as a third particle.

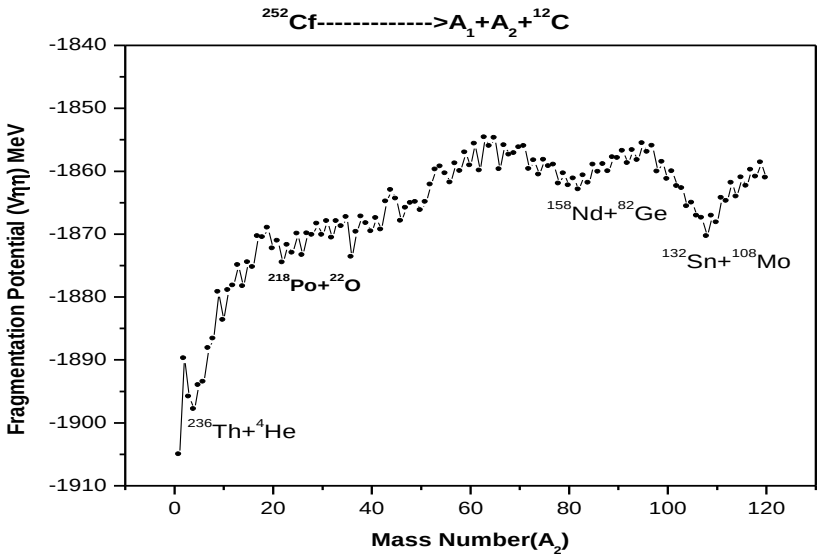

Figure 4.6 Fragmentation potential plotted with respect to A_2 for ^{12}C fixed as a third particle.

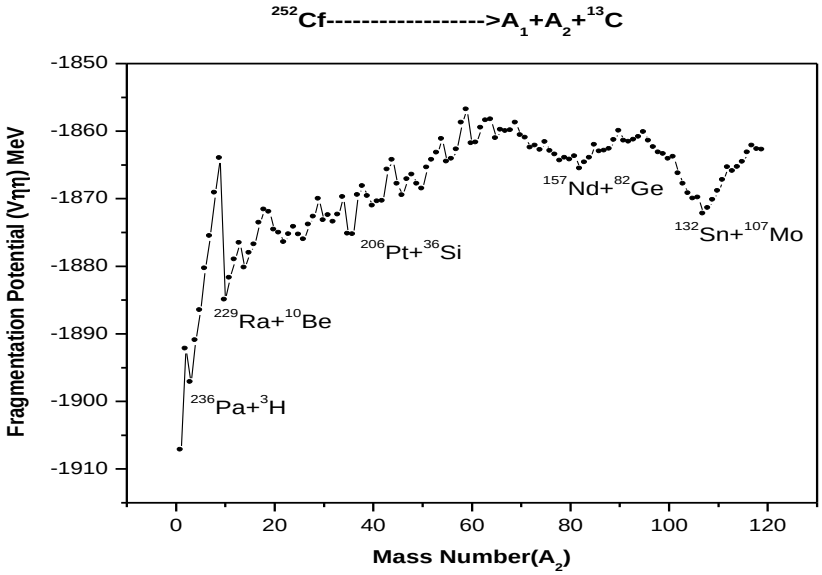

Figure 4.6 Fragmentation potential plotted with respect to A_2 for ^{13}C fixed as a third particle.

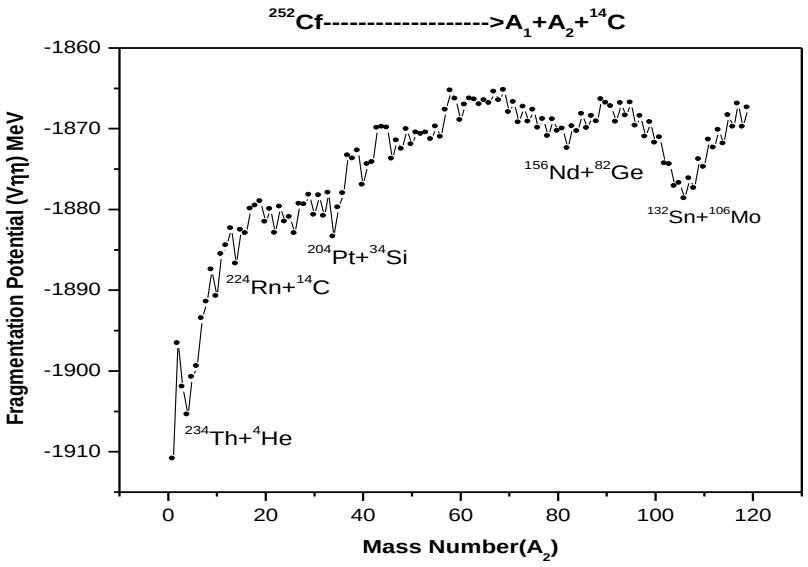

Figure 4.6 Fragmentation potential plotted with respect to A_2 for ^{14}C fixed as a third particle

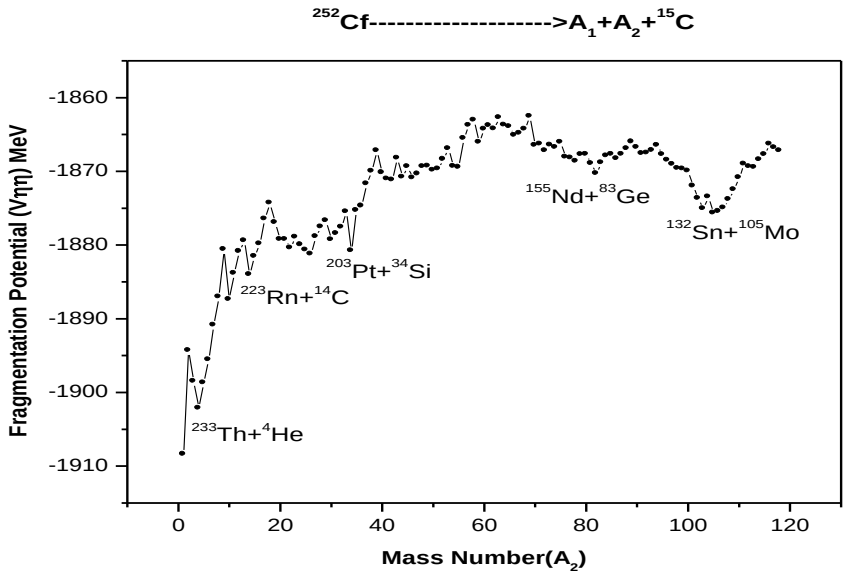

Figure 4.6 Fragmentation potential plotted with respect to A_2 for ^{15}C fixed as a third particle.

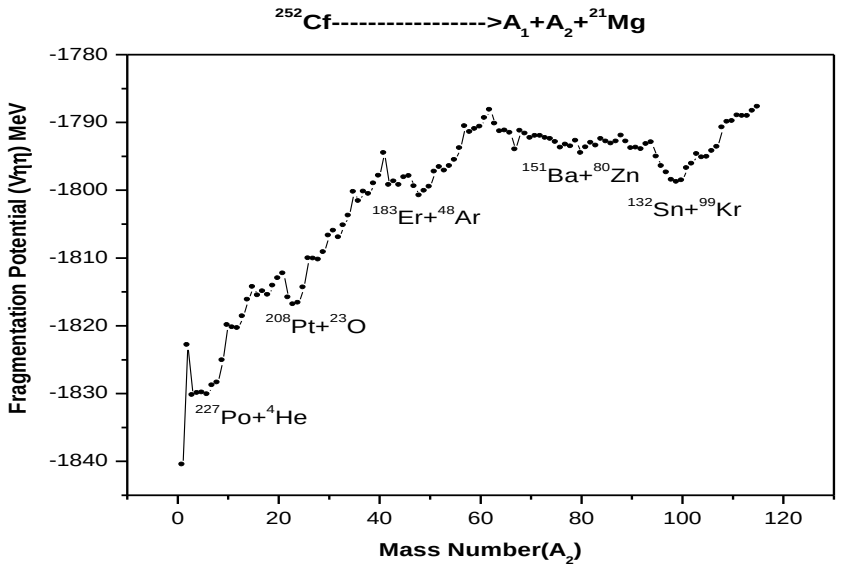

Figure 4.6 Fragmentation potential plotted with respect to A_2 for ^{21}Mg fixed as a third particle.

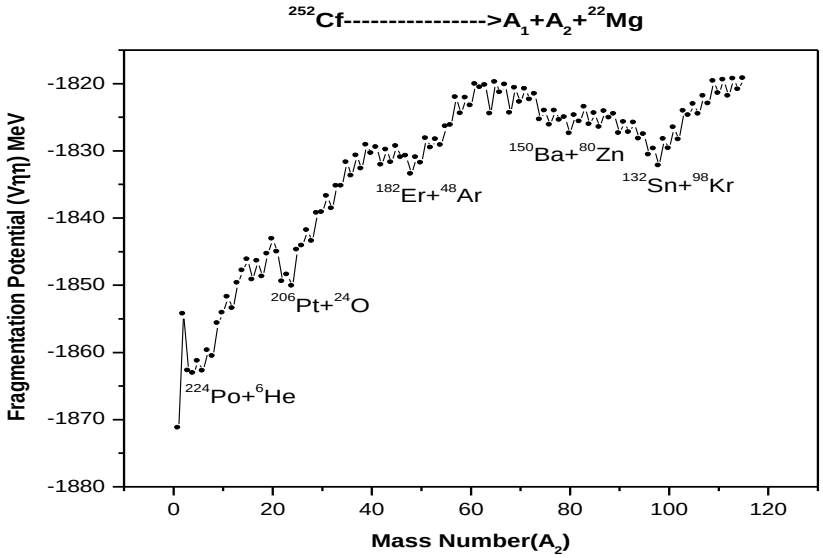

Figure 4.6 Fragmentation potential plotted with respect to A_2 for ^{22}Mg fixed as a third particle.

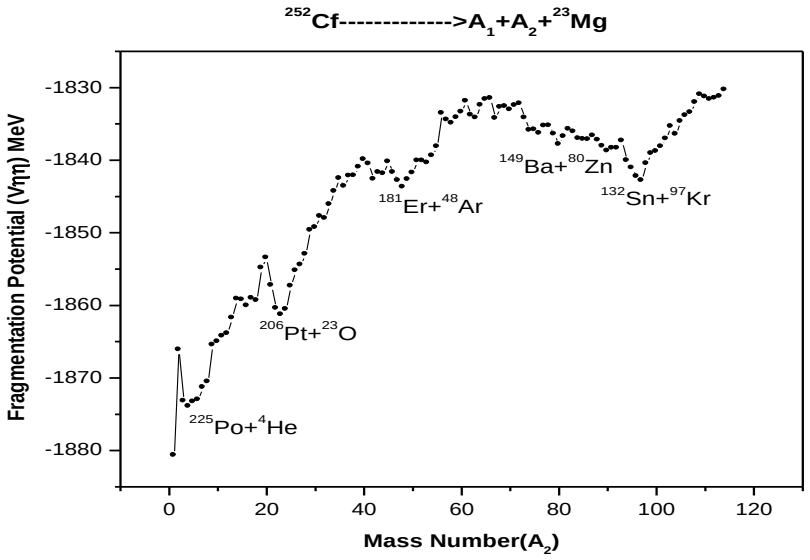

Figure 4.6 Fragmentation potential plotted with respect to A_2 for ^{23}Mg fixed as a third particle.

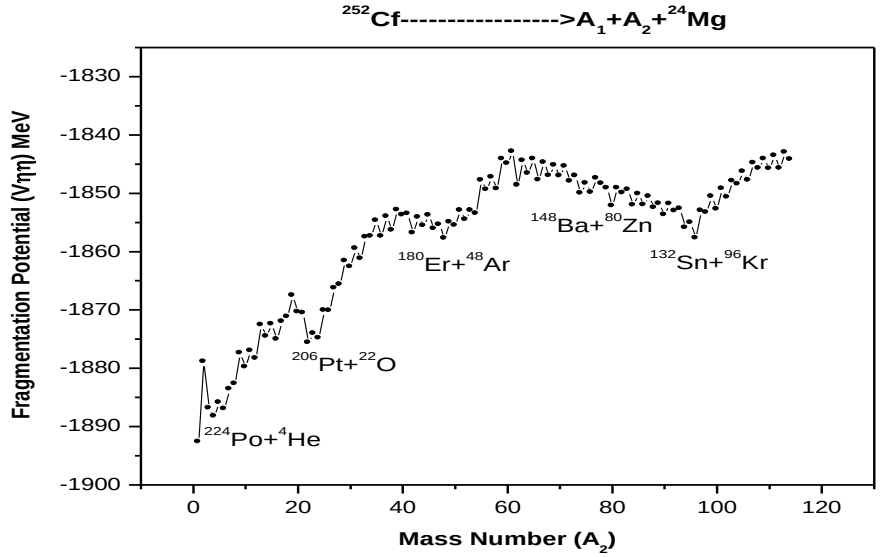

Figure 4.6 Fragmentation potential plotted with respect to A_2 for ^{24}Mg fixed as a third particle.

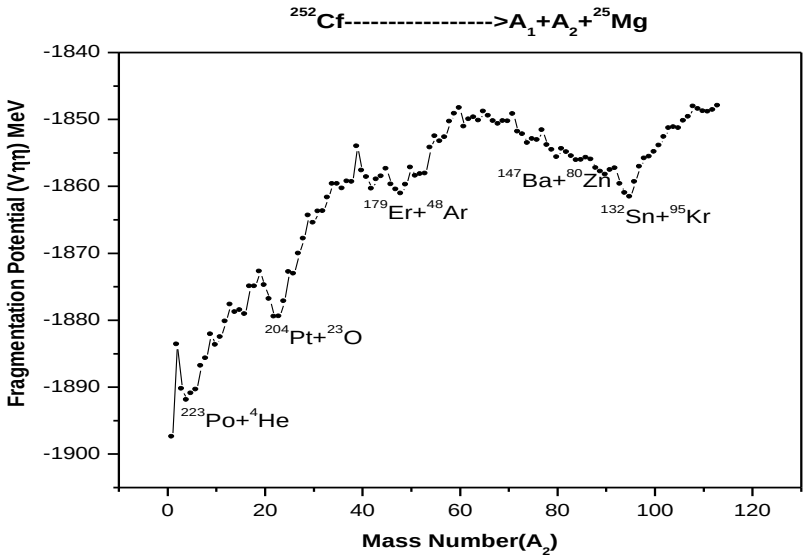

Figure 4.6 Fragmentation potential plotted with respect to A_2 for ^{25}Mg fixed as a third particle.

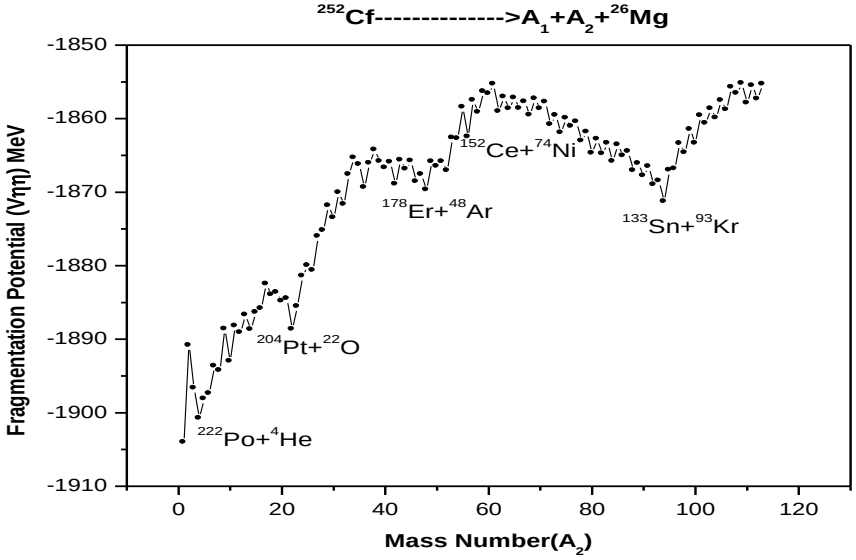

Figure 4.6 Fragmentation potential plotted with respect to A_2 for ^{26}Mg fixed as a third particle.

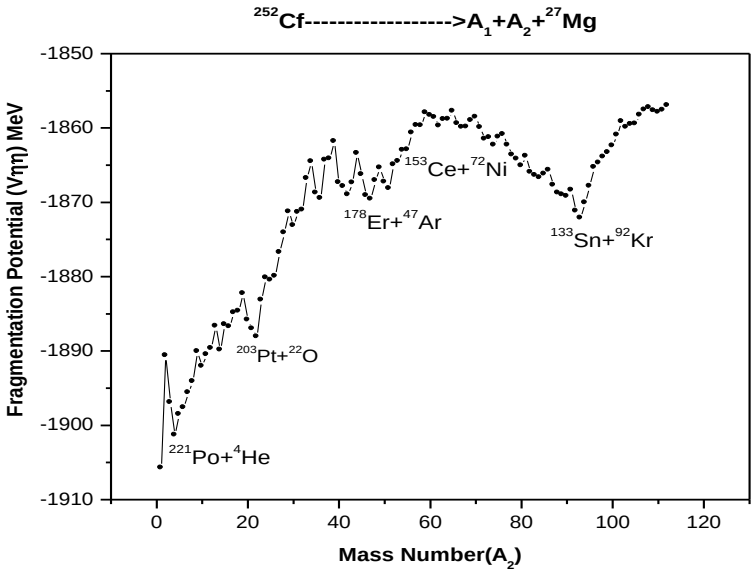

Figure 4.6 Fragmentation potential plotted with respect to A_2 for ^{27}Mg fixed as a third particle.

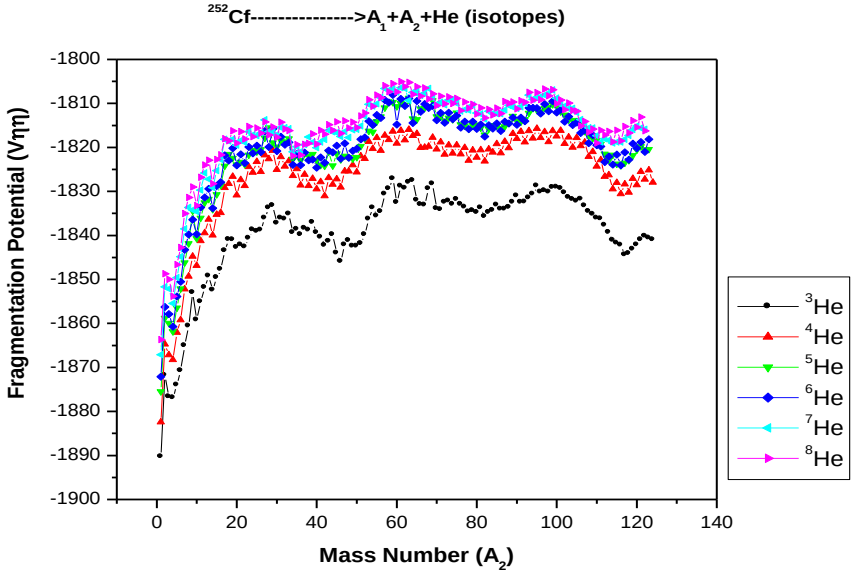

Figure 4.28 Fragmentation potential for the ternary decay of 252Cf with respect to A2 for He isotopes fixed as a third particle

.

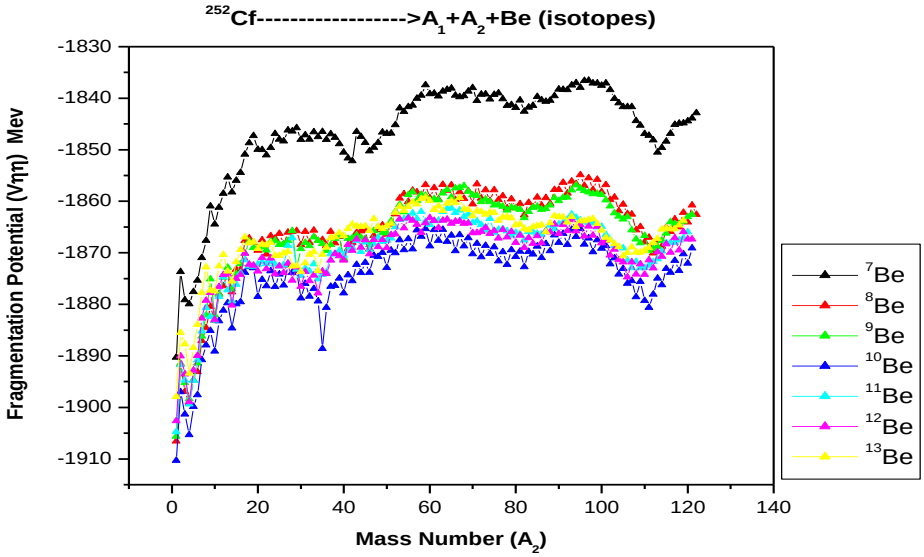

Figure 4.28 Fragmentation potential for the ternary decay of 252Cf with respect to A2 for Be isotopes fixed as a third particle.

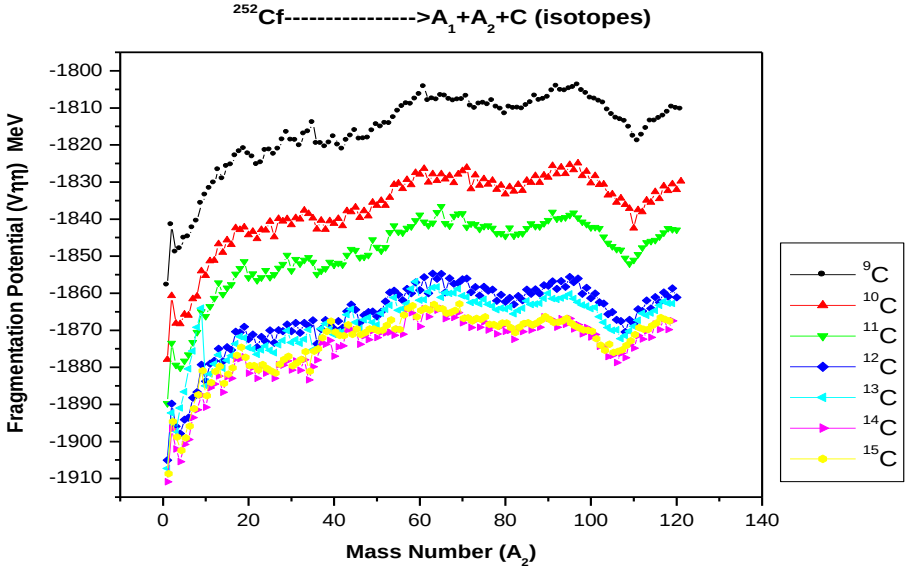

Figure 4.28 Fragmentation potential for the ternary decay of 252Cf with respect to A2 for C isotopes fixed as a third particle.

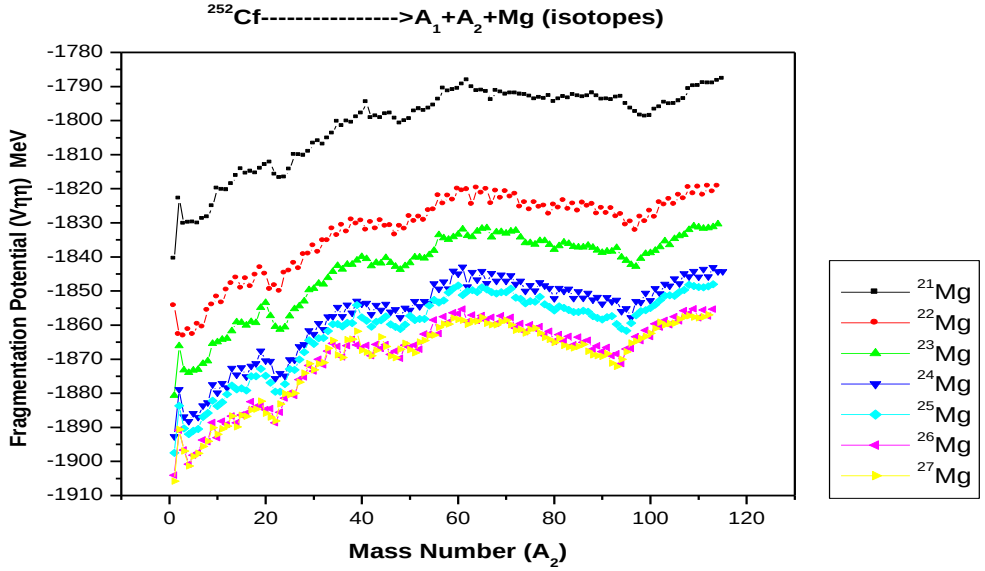

Figure 4.28 Fragmentation potential for the ternary decay of 252Cf with respect to A2 for Mg isotopes fixed as a third particle.

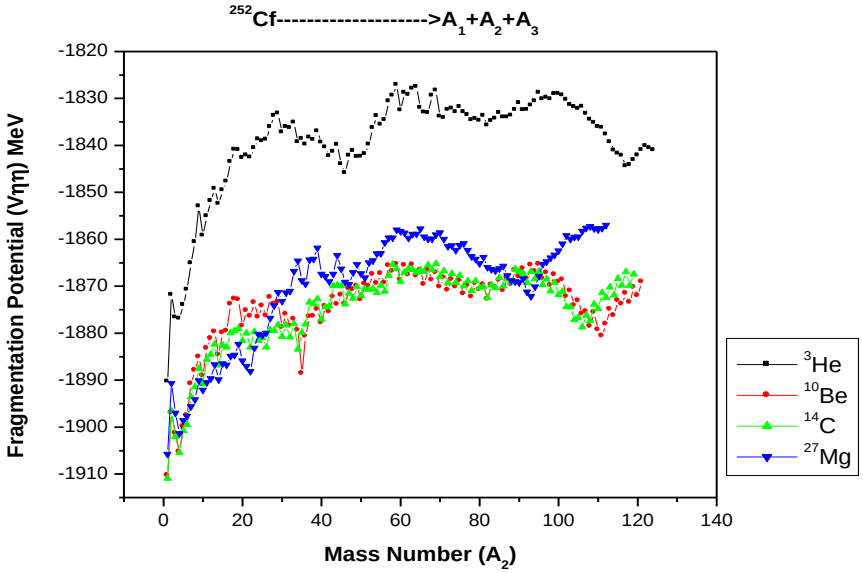

Figure 4.32 Fragmentation potential for the ternary decay of ^{252}Cf with respect to A_2 for ^{3}He, ^{10}Be ,^{14}C, Mg^{27} fixed as a third particle.

References

[1]. K. Manimaran and M. Balasubramaniam, Physical Review C, **79**, 024610 (2009).

[2]. J.H. Hamilton et al , Phys. At. Nuclei **65,** 645 (2002).

[3]. D.N. Poenaru, W Greiner, A.V. Ramayya, E .Hourany et al., Phys. Rev.C **59,** 3457 (1999)

[4]. D.N. Poenaru, B. Dobrescu, W Greiner, J.H. Hamilton andA.V.Ramayya, J.Phys. G: Nucl. Part. Phys.**26,** L97 (2000).

[5]. Yigal Ronen, Annals of Nuclear energy,**29,** 1013 (2002).

[6]. K. Manimaran, and M. Balasubramaniam, Physical Review C, **83,** 034609 (2011).

CHAPTER-V
SUMMARY AND CONCLUSION

In nuclear physics, nuclear fission is either a nuclear reaction or a radioactive decay process in which the nucleus of an atom splits into smaller parts (lighter nuclei). The fission process often produces free neutrons and photons (in the form of gamma rays), and releasing a very large amount of energy even by the energetic standards of radioactive decay. Fission is a form of nuclear transmutation because the resulting fragments are not the same element as the original atom. The two nuclei produced are most often of comparable but slightly different sizes, typically with a mass ratio of products of about 3 to 2, for common fissile isotopes. Most fissions are binary fissions (producing two charged fragments), but occasionally (2 to 4 times per 1000 events), three positively charged fragments are produced, in a ternary fission.

The breakup of a radioactive nucleus into three fragments covers a spectrum of fission events from one end in which a scission neutron accompanies two main fission fragments to the other end in which three fragments of about equal masses are emitted. Fragmentation potential is calculated using three cluster model (TCM) by calculation the binding energy (BE), of the three fragments along with the proximity potential (V_p), and coulomb potential (V_c), of the possible combination. The fragmentation potential is calculated for ternary fission of ^{252}Cf with third particle such as He isotopes (^{3}He,^{4}He,^{5}He,^{6}He,^{7}He,^{8}He), Be isotopes (^{7}Be,^{8}Be,^{9}Be,^{10}Be,^{11}Be,^{12}Be,^{13}Be), C isotopes (^{9}C,^{10}C,^{11}C,^{12}C,^{13}C,^{14}C,^{15}C) and Mg isotopes (^{21}Mg,^{22}Mg,^{23}Mg,^{24}Mg,^{25}Mg,^{26}Mg,^{27}Mg).

Among the He isotopes the most preferred one is ^{3}He. in the Be isotopes the most preferred one is ^{10}Be and in the C isotopes the most preferred one is ^{14}C and finally in the Mg isotopes, the most preferred one is ^{27}Mg. It is concluded that among the various isotopes as the third particles, ^{10}Be is found to be preferred third particle for the ternary decay of ^{252}Cf. Further the work can be extended to study the Preformation probability and life time of the ternary decay of experimentally measured data for ^{252}Cf.